

Seismic Tomography

Theory and practice

Edited by

H.M. Iyer

Geophysicist, US Geological Survey, Menlo Park, CA 94025

and

K. Hirahara

*Associate Professor, Disaster Prevention Research Institute,
Kyoto University, Japan*



CHAPMAN & HALL

London • Glasgow • New York • Tokyo • Melbourne • Madras

Refraction and wide-angle reflection tomography: theory and results

R.L. Nowack and L.W. Braile

26.1 INTRODUCTION

In this chapter, we present a review of seismic refraction and wide-angle reflection tomography. The classical meaning of tomography was originally the reconstruction of internal properties of an object from a complete angular set of line averages. However, today the term is often used in a more general sense for any procedure to mathematically reconstruct an internal property of an object using remotely recorded data. Seismic tomography using refraction data and wide-angle reflection data involves non-coincident sources and receivers, with receivers typically located at the Earth's surface. The seismic data set can be the entire seismic wavefield, or some subset of the data, such as travel times or amplitudes of selected phases. Refraction tomography implicitly relies on the heterogeneity of the medium to turn seismic energy back up to receivers at the Earth's surface. For smoothly varying media with interfaces this requires diving rays as well as rays that are reflected and refracted at interfaces.

Many experimental geometries can be used to image subsurface structure. Tomographic imaging using transmitted rays from distant sources (Figure 26.1(a)) or using reflected waves from nearly coincident sources and receivers (Figure 26.1(b)) produces limited angular ray coverage of the subsurface. Limited ray coverage is also common in cross-borehole geometries when using direct arrivals (Goulet, Chapter 29). In contrast, the use of refraction and wide-angle reflection data can provide a much broader range of angular ray coverage of the subsurface (Figure 20.1(c)), particularly when precritical reflections are included. Using multiple sources and receivers, this wide range of angular ray coverage can produce an increased resolution of the subsurface velocity structure. However, the ability to identify and correlate precritical as well as wide-angle reflections on refraction data generally requires a small receiver spacing (on the order of 0.1λ , where λ is the seismic wavelength), particularly in the near-source region of the recording profile (e.g. Braile and Chiang, 1986; Jarchow *et al.*, 1990).

The objectives of this paper are to present a brief review of previous applications of wide-angle tomography, to give an overview of the theory, and to provide several recent

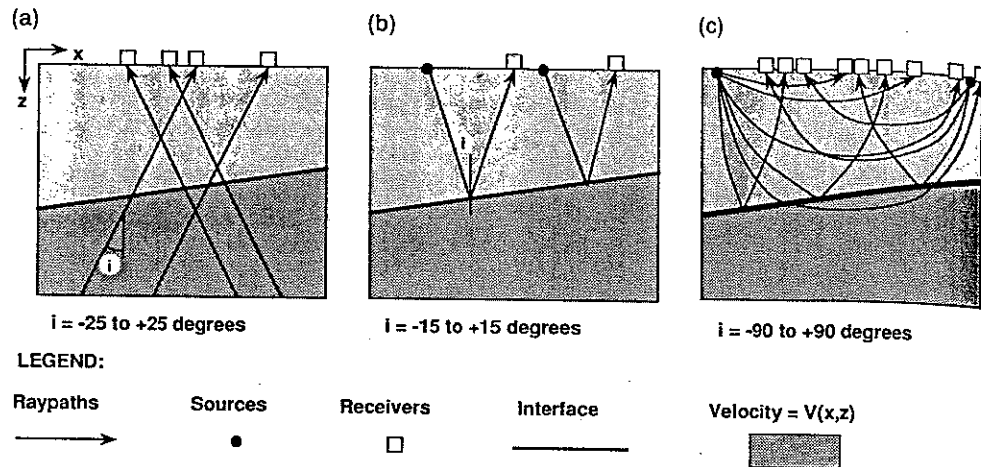


Figure 26.1 Schematic diagram of experimental geometries for seismic imaging. (a) Transmitted waves from distant sources recorded at receivers along the surface. (b) Reflected waves recorded from nearly coincident sources and receivers along the surface. (c) Refracted and wide-angle reflected waves with a broad range of angular ray coverage of the subsurface.

examples of tomographic imaging results. The emphasis is on crustal and uppermost mantle applications using both refraction and wide-angle reflection data. Also, emphasis is given to results in laterally varying media, with only a brief overview of the many one-dimensional (1-D) inversion results. End-member cases, such as near-vertical reflection and surface wave tomography are discussed elsewhere in this book as are applications involving teleseismic tomography.

26.2 HISTORICAL REVIEW

In this section, we present a brief review of wide-angle seismic applications of inversion and tomography to the Earth's crust and uppermost mantle. Wide-angle seismic inversion techniques differ in model complexity (one-, two- or three-dimensional (1-, 2- and 3-D) velocity variations), model parameterization, source and receiver geometry, and numerical solution method. Schematic illustrations of different techniques are shown in Figure 26.2.

The inversion of seismic refraction travel time data dates back to the work of Herglotz (1907) and Wiechert (1910) who inverted for radially varying velocity structure. The Herglotz–Wiechert method is written in terms of Abel transforms and assumes a smooth, radially varying medium with no low-velocity zones (Aki and Richards, 1980). The complete travel time curves must be used, including secondary triplications, for a unique solution. For example, Healy (1963) showed that non-uniqueness in the solution occurs when only first arrivals are used. The use of the travel time derivative, $dT/dx = p$, with distance, or alternatively using p with intercept time τ has the benefit of unwrapping triplications in the travel time data. Bessonova *et al.* (1974) gave inversion results in terms of $\tau(p)$, as did Garmany *et al.* (1979).

The classical tomography problem of reconstructing medium properties from a complete angular set of averages along straight lines can be written in terms of Radon transforms (e.g. Deans, 1983; Chapman, 1987). For straight rays in a radially concentric

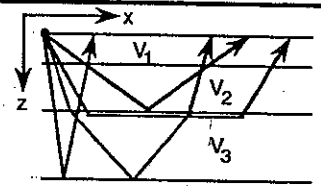
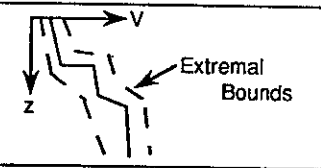
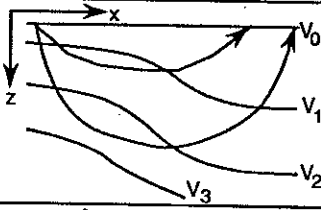
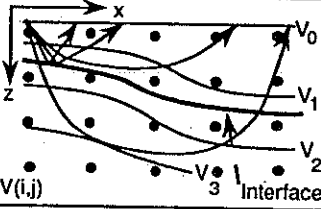
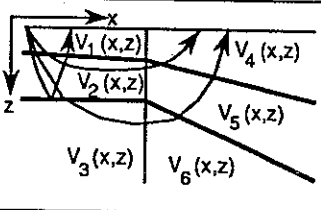
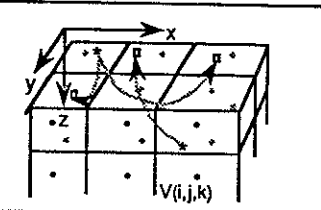
Method/Parameterization	Dim.	Model Illustration	Observed Data (Phases)
A. T-X Inversion; Homogeneous Layers	1-D		Refracted and Reflected Arrivals
B. Tau-p, Extremal Inversion; Slant Stack; $V(z)$ inversion	1-D		Refractions, (Wide-angle Reflections)
C. Iterative Ray Trace, $V(x,z)$ Polynomial	2-D		Refractions
D. Iterative Ray Trace, Velocity defined at node points $V(i,j)$, Interfaces may be included	2-D		Refractions and Reflections
E. Iterative Ray Trace, Velocity model defined by blocks and interfaces, $V(z)$ within blocks	2-D		Refractions and Reflections
F. Iterative Ray Trace, Velocity defined by homogeneous blocks or interpolated from nodes, $V(i,j,k)$	3-D		Controlled Source and Earthquake arrival times; Teleseismic delay times (transmitted case)

Figure 26.2 Seismic inversion methods, model parameterization, and typical observations.

medium, Radon transforms reduce to Abel transforms (Vest, 1974; Deans, 1983). Nowack (1990) noted that the Herglotz-Wiechert method which utilizes Abel transforms can be considered a specialized tomography-like algorithm along curved rays in a radially varying medium. Applications of seismic tomography may, therefore, be said to date back to the early part of this century.

In the presence of low-velocity zones, useful inversion results can still be obtained from travel time data in terms of bounds on the feasible solutions (Slichter, 1932; Gerver and Markushevich, 1967; Aki and Richards, 1980). None the less, blind spots due to low-velocity zones place limitations on refraction tomography results for vertically varying as well as more general, laterally varying media. For media with interfaces, precritical reflection data can reduce non-uniqueness in the solution when low-velocity zones are present.

Applications of generalized inversion methods to refraction travel time data for vertically varying media include the works of Kennett (1976), Kennett and Orcutt (1976) and Orcutt (1980). Braile (1973) presented a generalized inverse solution of both refraction and wide-angle reflection travel times in a horizontally stratified medium. Diebold and Stoffa (1981) investigated horizontally and dipping layered media.

Slowness-intercept transformations, or slant stacks, can be applied directly to seismic waveform data (McMechan and Ottolini, 1980; Chapman, 1981; Stoffa *et al.*, 1981; Phinney *et al.*, 1981; Stoffa, 1989). Slant stacked wavefields can then be iteratively inverted for vertical velocity structure (Clayton and McMechan, 1981). Inversions of wavefield data for 1-D structure using generalized inversion methods were performed by Shaw and Orcutt (1985) and Chapman and Orcutt (1985).

In laterally varying media, a specialized geometry using variable source and receiver time terms and an unknown refractor velocity was first investigated by Scheidegger and Willmore (1957) using a least squares approach called the time-term method. This method has been used in both shallow refraction seismics as well as crustal seismology (e.g. Willmore and Bancroft, 1960; Bamford, 1972). An extension of the time-term method to anisotropy was given by Raitt *et al.* (1969) for upper mantle velocity variations beneath the Pacific ocean. Ocola (1972) developed a non-linear least squares method for mapping laterally varying refractors. Hearn and Clayton (1986) also extended the time-term method by inverting for laterally varying crustal refractor velocities as well as time terms in southern California.

Alekseev *et al.* (1971) performed a linearized inversion of refraction data for smooth, laterally varying upper mantle structure from Pamir to Baikal in the Soviet Union (see also Alekseev *et al.*, 1990). Theoretical analysis of the ill-posed, linearized inverse problems in smooth, laterally varying media was performed by Romanov (1974) and Romanov and Alekseev (1980). Wesson (1971) investigated the least squares inversion of travel time data for smooth, laterally varying crustal structure at Bear Valley and Borrego Mountain in California. Other examples of linearized, kinematic inversion for laterally varying media using refraction data are given by Novotny (1981) and Firtas (1981, 1987).

Crosson (1976) performed a simultaneous inversion for 1-D Earth structure and hypocentral parameters. Aki and Lee (1976) simultaneously determined hypocentral parameters and laterally varying velocity in a block model using travel times from local earthquakes along the San Andreas fault in central California. Additional examples of simultaneous inversions for Earth structure and hypocentral parameters for local

earthquakes as well as shots include Chou and Booker (1979), Pavlis and Booker (1980), Thurber (1983), Benz and Smith (1984), Ankeny *et al.* (1986), Sambridge (1990) and Thurber (Chapter 20).

In this chapter, seismic inversion for laterally varying Earth structure from wide-angle data with known sources will be emphasized. These applications can involve controlled sources, earthquake sources with well-constrained hypocentral parameters, or cases in which a parameter separation technique has been applied (Thurber, Chapter 20). Further recent examples and applications of the inversion of seismic refraction data are given in Section 26.4.

26.3 REVIEW OF THEORY

Various inversion methods can be used to estimate subsurface seismic structure depending on the specific model parameterization and the scale and geometry of the velocity structure. With limited knowledge of the spectral characteristics of the medium, a wide range of the length scales should be anticipated. However, because of the difficulty in directly solving wide-band seismic inversion problems, a two-scale approach is often used. The long-wavelength or smoothly varying components of the medium are estimated first and the short-wavelength features second. There is some similarity here with reflection seismology where velocity analysis determines the smoothly varying components of the medium followed by stacking and migration (using the derived velocity model) to estimate the short-wavelength components of the medium. However, in the reflection case, the long-wavelength information from the velocity analysis is not included in the final image.

The two-scale approach to seismic inversion is complicated by the fact that the estimation of smoothly varying medium parameters can be contaminated by effects of the small-scale structures. For example, for an isotropic medium with small-scale layering, a smoothly varying inversion could indicate effective anisotropy and possibly anelasticity. However, bias resulting from small-scale features can ultimately be adjusted when an inversion for small-scale structure is performed. A separation between smoothly varying and fine-scale structure can be made based on the dominant seismic wavelength of the source.

For smoothly varying media, as compared with the dominant seismic wavelength, ray theoretical methods and their extensions can be applied. Kravtsov and Orlov (1990) describe the conditions under which ray methods are generally applicable. Physically, seismic rays are the trajectories along which high-frequency energy flows. The size of the first Fresnel zone can be used as an estimate of the effective width along a ray (Nolet, 1987; Kravtsov and Orlov, 1990). Because ray methods can be used directly to compute travel times and ray amplitudes, it is natural to apply inversions to these quantities.

The use of travel times and amplitudes of selected phases requires that these parameters be estimated from the observed seismic record sections. For seismic refraction data, travel times and amplitudes can be estimated manually and can be verified using methods such as reciprocity of travel times between shot gathers. Alternatively, automated algorithms to obtain travel times from wavefield data can be used (Allen, 1982; Zelt *et al.*, 1987). However, in the presence of 'noise', and for secondary arrivals, automated picking of travel times can be a difficult task. None the less, the quality of any inversion method using travel time and amplitude data is only as good as the procedure used to estimate these observables from the data.

Using ray methods, travel times can be considered as line averages of the medium slowness along curved ray trajectories. For the special case of straight ray-paths, the classical tomographic reconstruction of medium properties from line averages results. None the less, tomographic reconstruction techniques can be applied along either straight or curved rays depending on the geometry of the problem and the properties of the medium (e.g. Beylkin, 1984).

The ray method also can be applied to smoothly varying media with curved interfaces. Assuming that the interfaces are slowly varying, the reflected and transmitted rays can be computed by applying Snell's Law locally, computing reflection and transmission coefficients with respect to the local tangent plane, and correcting the geometric spreading along the ray for the curvature of the boundary. Head waves are not included in first-order ray methods with interfaces. For these waves, higher order ray methods, or decompositions in terms of plane waves or Gaussian beams, must be used (Červený, 1985a,b).

For the inversion of fine-scale structure of the medium, the first-order Born, or single scattering, approximation is often implemented using wavefield data. The Born approximation is valid when the scattered field is small compared with the incident field (Aki and Richards, 1980). Tarantola (1984, 1987) and Tarantola *et al.* (Chapter 28) formulated seismic inversion methods based on the Born approximation and related them to classical seismic migration algorithms for reflection data. Wavefield migration has been applied to wide-angle reflection, wavefield data by McMechan and Fuis (1987) and Chang and McMechan (1989a,b). However, care must be taken if multiple scattering is significant. Iterative inversion procedures must be used to account for multiple scattering effects. Particularly for refraction and wide-angle reflection data, large postcritical reflection coefficients can often lead to multiple scattering.

In the following subsections, we summarize ray-theoretical methods for smoothly varying media with curved interfaces, briefly discuss seismic inversion for small-scale structure using refraction data, and conclude with a brief discussion of generalized inversion techniques.

26.3.1 Ray-theoretical methods

To invert seismic refraction and wide-angle reflection data, partial derivative operators must be derived describing the sensitivity of the data to the model parameters. For ray methods, one relates the changes in travel times and ray amplitudes to corresponding changes in the wave speed, attenuation, and interface parameters. The travel time along a ray can be written

$$T = \int_{s_0}^s L(u(\mathbf{x}), \mathbf{x}, \dot{\mathbf{x}}) ds, \quad (26.1)$$

where \mathbf{x} is the position, s is the path length, $\dot{\mathbf{x}}_i = dx_i/ds$ and x_i is a component of \mathbf{x} . For an isotropic medium, $L = u(\mathbf{x})(\dot{\mathbf{x}}_i \dot{\mathbf{x}}_i)^{1/2}$ and $u(\mathbf{x})$ is the medium slowness. The first variation of the travel time for an isotropic medium can then be written

$$\delta T \approx \left. \frac{\partial L}{\partial \dot{\mathbf{x}}_i} \delta x_i \right|_{s_0}^s + \int_{s_0}^s \left(\frac{\partial L}{\partial x_i} - \frac{d}{ds} \frac{\partial L}{\partial \dot{\mathbf{x}}_i} \right) \delta x_i ds + \int_{s_0}^s \delta u(\mathbf{x}) ds, \quad (26.2)$$

(e.g. Nowack and Lyslo, 1989). For a geometric ray, with no slowness perturbations and fixed end-points, $\delta T = 0$. Using equation (26.2), the equations for the ray trajectories can be obtained from $\partial L / \partial x_i - d/ds (\partial L / \partial \dot{x}_i) = 0$.

For a ray with fixed end-points, the perturbation of the travel time due to a variation in the material slowness, $u(\mathbf{x})$, is given by the third term in equation (26.2). Thus, $\delta T \approx \int_{s_0}^s \delta u(\mathbf{x}) ds$, where to first order this is computed along the original, unperturbed ray-path. Using unperturbed rays, or rays from a previous iteration for the calculation of travel time derivatives results in major computational savings and is done in most travel time tomography algorithms. None the less, higher order perturbations of travel time perturbations of the ray trajectories are required.

For the smoothly varying components of the medium, a finite basis expansion can be written as

$$u(\mathbf{x}) = \sum_{j=1}^N \alpha_j h_j(\mathbf{x}),$$

where $h_j(\mathbf{x})$ are the basis functions and α_j are the coefficients. For example, Aki and Lee (1976) used rectangular blocks of constant velocity as basis functions. Dziewonski (1984) performed a travel time inversion for mantle heterogeneities using a global expansion in terms of spherical harmonics. For many applications, splines provide alternatives which are reasonably localized and result in continuous second derivatives. Alternatively, tetrahedra or finite cells can be used to represent the medium.

Given discrete data and a finite basis expansion for the medium, a discrete linearized inverse problem can be written as

$$\delta d_i = \sum_{j=1}^N G_{ij} \delta m_j + O(\delta m^2), \quad (26.3)$$

where for travel time data, $\delta d_i = T_i^{\text{obs}} - T_i^{\text{calc}}$, $i = 1, M$ and $\delta m_j = \alpha_j - \alpha_j^0$, $j = 1, N$. The sensitivity operator $G_{ij} = \int_{\text{ray}_i} h_j(\mathbf{x}) ds$ can be computed to first order along the unperturbed i th ray.

For highly non-linear problems, the linearization in equation (3.26) can be implemented within an iterative inversion procedure. For example, Tarantola and Valette (1982) describe an iterative least squares solution to non-linear inverse problems. For travel time tomography, each complete iteration requires ray-tracing in the updated velocity model as well as the recalculation of G_{ij} . Iterations proceed until no further improvement in the fit to the data results. Early applications of travel time tomography often included only one iteration, calling into question the ultimate convergence of the solution. Even now, multiple iterations may be prohibitive for certain large-scale problems.

The methods applicable to forward ray-tracing are dependent on the type of model parameterization (e.g. Červený, 1987). A direct numerical ray integration in terms of splines has been given by Červený and Pšenčík (1984) and Červený *et al.* (1988). For finite cells, ray algorithms which are analytic in each cell are faster than direct numerical algorithms (e.g. Virieux *et al.*, 1988). Alternatively, fast ray-tracing using perturbation methods in cells is described by Farra (1990) and Virieux (1991).

Figure 26.2 gives examples of methods for seismic inversion which are dependent on the type of medium parameterization. Figure 26.2(a) shows the inversion of 1-D homogeneous layers using refracted and reflected arrivals (Braille, 1973), and Figure 26.2(b) the inversion for 1-D continuously varying media (Bessonova *et al.*, 1974;

Kennett, 1976; Kennett and Orcutt, 1976; Orcutt, 1980; Diebold and Stoffa, 1981). Figure 26.2(c) illustrates the 2-D inversion for a smooth, functional representation of the medium using refracted waves (Wesson, 1971). Figure 26.2(d) displays the 2-D inversion of velocity defined at nodes. This approach includes splined node interpolation of the velocity (e.g. Lutter *et al.*, 1990) as well as splined interpolation of interfaces (Lutter and Nowack, 1990). Figure 26.2(e) shows the 2-D inversion for velocity defined by blocks or cells (Zelt and Smith, 1992). Finally, Figure 26.2(f) illustrates 3-D inversion for either blocks or interpolated nodes (Benz and Smith, 1984; Ankeny *et al.*, 1986; Kissling, 1988).

An alternative procedure for the computation of travel times is a direct, numerical solution of the eikonal equation (Vidale, 1988). This procedure can be very efficient computationally because the travel times can be computed in the coordinate space rather than the complete six-dimensional phase space of \mathbf{x} and the ray parameter vector, \mathbf{p} , required for ray-tracing. None the less, for wave front triplications, and other secondary arrivals, the travel time problem often requires a more complete solution (Nowack, 1992).

For anisotropic media, first-order variations in the travel time from a smoothly varying change in the medium can be written as

$$\delta T = -\frac{1}{2} \int_{\tau_0}^{\tau} \delta a_{ijkl} p_i p_j g_k^{(m)} g_l^{(m)} d\tau, \quad (26.4)$$

where δa_{ijkl} is the change in the density normalized stiffness parameters, p_i is the ray parameter vector and $g_j^{(m)}$ is the particle motion vector for the m th wave (Červený and Jech, 1982; Hanyga, 1982; Červený and Fírbas, 1984; Hirahara, Chapter 18). For an initial isotropic medium with degenerate S waves, equation (26.4) must be modified according to Jech and Pšenčík (1989). Nowack and Pšenčík (1991) extended this method to the perturbation of ray trajectories. Gajewski and Pšenčík (1989) developed a general computer code for anisotropic ray-tracing. Anisotropic modeling may be required even within inversions for isotropic media if fine-scale structure aliases into longer wavelength anisotropy.

For a geometric ray which is reflected or transmitted from a curved boundary, the first term in equation (26.2) can be used to find the travel time perturbation. Thus,

$$\delta T \approx \frac{\partial L}{\partial \dot{x}_i} \delta x_i \bigg|_{s_a^-}^{s_a^+} = p_i \delta x_i \bigg|_{s_a^-}^{s_a^+},$$

where s_a^- is for the incident ray and s_a^+ is for the reflected/transmitted ray. This expression can be used to obtain the variation in the travel time due to a perturbation in the boundary shape,

$$\frac{\partial T}{\partial h(x_a)},$$

where $h(x_a)$ is the vertical boundary position at the point of incidence. It is a first-order approximation because it assumes a slowly varying material slowness of velocity near the boundary.

The interface perturbation at the point of incidence x_a can be related to a node perturbation of an interpolated boundary. Using splines for example, the coefficients

for a perturbation of an interface node can be computed, and from these the values of

$$\frac{\partial h(x_a)}{\partial z(x_{\text{node}})}$$

can be found. The first variation of travel time with respect to a perturbation of a boundary node of an interface can then be written

$$\delta T \approx \frac{\partial T}{\partial h(x_a)} \frac{\partial h(x_a)}{\partial z(x_{\text{node}})} \delta z(x_{\text{node}}), \quad (26.5)$$

(Nowack and Lyslo, 1989). For the special case of a piecewise linear boundary and an incident reflected ray, this reduces to the results given by Bishop *et al.* (1985). Equation (26.5) can then be formulated as a linearized inverse problem similar to equation (26.3) for reflected and transmitted wave travel times and the node depths for each interface.

In the ray-theoretical approximation, the seismic amplitude, $\hat{U}(O_s)$, of a multiply reflected and transmitted ray can be written (see Červený, 1985a,c, 1992)

$$\hat{U}(O_s) = A(O_s) \hat{C}(O_s) \prod_{i=1}^N [\hat{R}(O_i) \hat{G}(O_i)] \hat{\Psi},$$

where \hat{C} is the receiver matrix, \hat{R} is the reflection/transmission matrix, $\hat{\Psi}$ is the source matrix, and \hat{G} is the rotation matrix at each interface. $A(O_s)$ contains the geometric spreading and can be written

$$A(O_s) = \frac{1}{[V(O_s)\rho(O_s)\det Q(O_s)]^{1/2}} \prod_{i=1}^N \left[\frac{V'(O_i)\rho'(O_i)\det Q'(O_i)}{V(O_i)\rho(O_i)\det Q(O_i)} \right]^{1/2},$$

where O_s is the receiver position, O_i is the i th reflection/transmission point, $v(O_i)$ is the velocity and $\rho(O_i)$ is the density. The unprimed values are on the incident ray side of the boundary and the primed values are on the reflected/transmitted side. $Q(O_s)$ is a 2×2 matrix derived from

$$X(O_s) = \begin{bmatrix} Q(O_s) \\ P(O_s) \end{bmatrix} = \pi(O_s, O_N) \prod_{i=N}^1 [F(O_i) \pi(O_i, O_{i-1})] X(O_0),$$

where $\pi(O_i, O_{i-1})$ are the component ray propagator solutions to the dynamic ray equations for each layer with $\pi(O_i, O_i) = I$ (Červený, 1985a). $F(O_i)$ is the transformation matrix at each interface. For suitable initial conditions, $\det Q(O_s)$ will be the geometric spreading for a point source.

Perturbation theory of the dynamic ray equations has been developed by Farra and Madariaga (1987). Approximate two-point ray-tracing can be performed using perturbation theory. It can be used also to compute perturbed ray amplitudes due to variations in the medium. Partial derivatives of ray-theoretical amplitudes have been tested in trial inversions by Nowack and Lutter (1988a) for smoothly varying media and by Nowack and Lyslo (1989) for media with smoothly varying interfaces. Once the partial derivatives of ray amplitude have been derived, a linearized inverse problem similar to equation (26.3) using ray amplitude can be implemented for variations in the medium velocity or slowness.

Ray methods for slightly dissipative media have been described by Červený and Frangie (1982) (Červený, 1992). The seismic response of 2-D absorbing structures was computed using the ray method of Moczo *et al.* (1987). Tonn (1991) compared different

methods for estimating Q . Evans and Zucca (1988) performed an inversion for attenuation in the Medicine Lake Volcano region of California using spectral ratios. Jacobson and Lewis (1990) performed inversions for Q structure in the shallow ocean crust. Nowack and Trehu (1989) implemented a seismic pulse inversion in which travel time, amplitude, and pulse broadening of a time-domain pulse were used to invert for both seismic velocity and attenuation beneath Lake Superior. For other examples of attenuation tomography see Evans and Zucca (Chapter 25) and Sanders (Chapter 24).

In singular regions, such as caustics and at critical distances, extensions of the ray method are required. Recent extensions include the Gaussian beam method (Popov, 1982; Červený *et al.* 1982; Nowack and Aki, 1984; Červený, 1985b) as well as the Maslov method (see Chapman and Drummond, 1982; Chapman, 1985; Thompson and Chapman, 1985). Modeling of edge diffractions has also been incorporated (Klem-Musatov and Aizenberg, 1984; Pedersen *et al.*, 1989). Macdonald *et al.* (1987) has shown that extensions to the ray method are required to model and invert amplitude data accurately for wide-angle reflected waves near the critical distance.

26.3.2 Full wavefield methods

For fine-scale structure of the medium with respect to the dominant wavelength of the source, wave scattering and diffraction effects become important. Williamson (1991) suggested, based on a comparison of diffraction and travel time tomography, that diffraction effects become important for medium scales smaller than the radius of the first Fresnel zone along the ray trajectories. The first Fresnel zone radius has been used to define the effective width of rays at finite frequencies (Kravtsov and Orlov, 1990; see also, Nolet, 1987).

For scales of the medium smaller than the dominant seismic wavelength, the most straightforward inversion procedure is to directly perform an iterative linearization in terms of the seismic wavefield. As an example, the Fourier transformed wave equation can be written as, $\nabla^2 u(\underline{x}) + k^2(\underline{x})u(\underline{x}) = -s(\underline{x})$, where $u(\underline{x})$ is the field variable, $s(\underline{x})$ is the source term, $k^2(\underline{x}) = \omega^2/V^2(\underline{x})$, and $V(\underline{x})$ is the variable velocity of the medium. Let $u(\underline{x}) = u_0(\underline{x}) + \delta u(\underline{x})$ and $k^2(\underline{x}) = k_0^2(\underline{x}) + \delta[k^2(\underline{x})]$. Then to first order $\nabla^2 \delta u(\underline{x}) + k_0^2 \delta u(\underline{x}) = [2\omega^2/V_0^3(\underline{x})]\delta V(\underline{x})u_0(\underline{x})$. Using the Green's function for the initial medium, this can be written

$$\delta u(\underline{x}_r) = - \int \left[G(\underline{x}', \underline{x}_r) \frac{2\omega^2}{V_0^3(\underline{x}')} u_0(\underline{x}', \underline{x}_s) \right] \delta V(\underline{x}') d\underline{x}', \quad (26.6)$$

where $G(\underline{x}', \underline{x}_r)$ is the computed field for a point-source located at the receiver location, \underline{x}_r , and evaluated at the medium point, \underline{x}' . The forward field $u_0(\underline{x}', \underline{x}_s)$ is computed at the medium point for a source at \underline{x}_s . The quantity in brackets in equation (26.6) is the first-order sensitivity operator giving the variation of the wavefield due to a change in the velocity model, $\delta V(\underline{x})$. For the inverse problem, $\delta u(\underline{x})$ can be written as the observed field minus the field computed for the initial model. This formulation has been investigated by Tarantola (1984, 1987) who found that a steepest descent solution using the adjoint sensitivity operator was kinematically similar to a sequence of Kirchhoff migrations for the wave equation (see also, Nowack and Aki, 1986). The first iteration is equivalent to that used in conventional seismic reflection processing of CMP data. The resulting imaging criterion was found to be similar to that of Claerbout (1971, 1976). The first iteration is a single scattering approximation, but higher iterations allow for multiple scattering to be included in the inversion, assuming that the Green's

functions can be computed accurately. Tarantola (1987) gives analogous sensitivity operators for the elastic wave equation.

For wide-angle seismic applications, a Kirchhoff, prestack type of migration was implemented by McMechan and Fuis (1987) for wide-angle reflection data from southern Alaska. However, for this case there was evidence of multiple scattering (Flueh *et al.*, 1989). Other examples of wavefield processing of wide-angle seismic data include Chang and McMechan (1989a,b). Pan and Phinney (1989) developed an iterative inversion of wavefield data for a vertically varying medium. Sun and McMechan (1991) performed an iterative, full waveform inversion using synthetic, wide-angle SH data, and were able to recover the higher wave-number components of the medium assuming the long wave-number components were given a priori. Wavefield inversions using refraction data with sensitivity operators computed using the WKBJ approximation have been given by Shaw and Orcutt (1985) and Chapman and Orcutt (1985). Shaw (1988) performed a waveform inversion of static-time-corrected refraction data.

Extensions of seismic waveform inversions by a linearization of the logarithm of the wavefield, the Rytov approximation, have been suggested by Nowack and Aki (1986). These extensions allow some forward multiple scattering (Keller, 1969). Numerical examples for simple layered cases are given by Oristaglio (1985) who shows certain advantages of the Rytov approximation for the simple transmission case (see also, Beydoun and Tarantola, 1988). Further work on wavefield inversions is required to find the best iterative linearization procedures.

26.3.3 Methods for generalized inversion

A variety of generalized inversion procedures can be applied to discrete geophysical inverse problems. In seismology, most inverse problems are ill-posed and include non-uniqueness in the solution and incomplete and inaccurate data. One of the methods of solution is the natural inverse of Lanczos (Lanczos, 1961; Jackson, 1972; Wiggins, 1972; Aki and Richards, 1980) based on the singular value decomposition. However, even using the natural inverse of Lanczos, small but non-zero singular values can have a large effect on the resulting solution. One approach to stabilize the natural inverse solution has been to eliminate small singular values below some critical value.

A variety of methods of stabilizing generalized inverse solutions have been developed. These include damped least squares, stochastic inversion (Franklin, 1970), Bayesian inversion (Jackson and Matsu'ura, 1985; Duijndam, 1988) as well as the non-linear stochastic formulation of Tarantola and Valette (1982). For stochastic inversions, a priori model and data covariance operators are used to damp as well as smooth the generalized inverse solution. For example, diagonal elements of the a priori model covariance would act to constrain the inverse solution to the vicinity of the initial model. Alternatively, off-diagonal elements of the a priori model covariance provide a way to smooth the inverse model solution.

In addition to the inverse solution, a posteriori model errors and covariance as well as resolution should be estimated for all inversion techniques. These measures provide estimates of model reliability as well as the range of feasible solutions consistent with the data and the a priori information. For non-linear problems, only linearized estimates of the a posteriori model covariance can usually be determined (Tarantola, 1987; Nowack and Lutter, 1988b).

Because many geophysical inverse problems are non-linear, iterative solutions are usually required. The forward problem and the sensitivity operator must then be

recomputed for higher iterations. Iterations are continued until no significant improvement in the solution can be obtained. Lutter *et al.* (1990) used an iterative procedure using refraction travel times to estimate a smoothly varying velocity model in which a small number of velocity parameters was estimated first, followed by inversions for more detailed velocity models. In this way the longer wavelength components of the model were frozen into the solution during the first iterations. Williamson (1990) used a similar method to constrain long-wavelength medium components using reflection seismology.

In practice, standard methods for solving linearized inverse problems can be restrictively slow for large seismic tomography problems. For example, recent tomography studies for the mantle have had as many as 10^6 travel times and 10^4 – 10^5 unknown medium parameters (Dziewonski, 1984; Spakman and Nolet, 1988). For large sparse, linear inverse problems, several types of iterative matrix inversion techniques have been used. One class includes Algebraic Reconstruction Techniques (ART) and related Simultaneous Iterative Reconstruction Techniques (SIRT). These have been applied in medical imaging (Herman, 1980) and in geophysics (Dines and Lytle, 1979). A second class of solutions is based on a generalization of the conjugate gradient method. For example, the LSQR algorithm of Paige and Saunders (1982) can be applied to non-square, damped least squares problems. Geophysical applications have been described by Nolet (1985, 1987) and in Chapters 9 and 10, and Spakman and Nolet (1988). Van der Sluis and Van der Vorst (1987) found the LSQR algorithm to be generally superior to SIRT for many large tomographic problems. Nowack and Lutter (1988a) used LSQR to invert both travel times and ray amplitudes in trial inversions for seismic velocity. Techniques using subspace and projection methods for large-scale geophysical inverse problems have also been developed by Kennett and Williamson (1988).

26.4 EXAMPLES OF WIDE-ANGLE TOMOGRAPHY

In this section, several recent examples of refraction tomography are summarized. These include 1-D and 2-D inversion results from the 1986 Ouachita PASSCAL (Program for Array Seismic Studies of the Continental Lithosphere) experiment and the 1986 Nevada PASSCAL experiment. The 2-D inversion results using refraction data from the 1980 Yellowstone–eastern Snake River Plain experiment (Elbring, 1984) are described briefly. Finally, the inversion results of Ankeny *et al.* (1986) for the Jemez Mountains volcanic field, New Mexico, are shown as an example of 3-D seismic inversion of refraction data.

Keller *et al.* (1989) describe the geometry of the 1986 Ouachita experiment in southwestern Arkansas and northeastern Louisiana. Lyslo and Nowack (1990) used wavefield data from one shot gather to estimate the 1-D velocity profile in the central part of the deployment. They windowed and slant stacked the wavefield data using an approach similar to McMechan and Ottolini (1980) and Clayton and McMechan (1981). The slant stack wavefield was then downward continued to obtain the $\psi(z)$ wavefield shown in Figure 26.3. The solid line is their estimate of the 1-D velocity structure. This model is similar to ray trace results of Jardine (1988) and travel time inversion results of Lutter and Nowack (1990) for the Ouachita experiment. A full wavefield inversion has the advantage of not requiring the picking of travel times until the final step of the inversion process. Uncertainties of the estimated velocities can be inferred from the width of the zone of larger amplitudes in Figure 26.3.

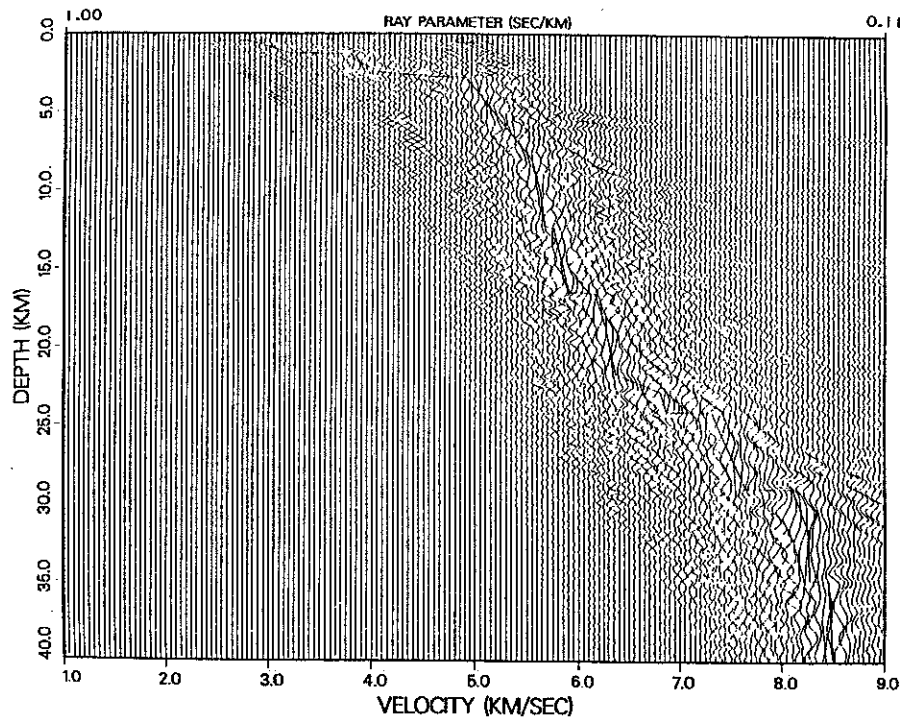


Figure 26.3 Velocity-depth, $v(z)$, wavefield image of the τ - p slant stacked data from shotpoint 16 of the 1986 Ouachita PASSCAL experiment (from Lyslo and Nowack, 1990).

Seismic inversions based on travel times require the picking of travel times from the wavefield data. Manual picking of travel times can be complicated when using data which are sparsely sampled with distance. Furthermore, adequate spatial sampling is essential for proper correlation of different phases. Even with adequate spatial sampling, the final inversion and interpretation of refraction results can be highly dependent on the travel time correlations that have been made and on the errors in the travel times. Lutter *et al.* (1990) used reciprocity of travel time on overlapping shot gathers to constrain the travel time correlations for first arrivals as well as secondary reflection phases. Visual correlations are also enhanced by using reduction velocities that flatten the corresponding phase on reduced wavefield record sections.

Examples of automated travel time picking algorithms include those developed by Allen (1982) and Zelt *et al.* (1987). Figure 26.4 shows an example of automated phase correlation on observed refraction data from Zelt *et al.* (1987). Automated phase correlation of seismic data sets with significant noise levels as well as sparse sampling can be a difficult task. For refraction and wide-angle data, such picking is complicated by progressive phase shifts and change of pulse character. Lyslo (1988) found for wide-angle Moho reflections from the Ouachita PASSCAL experiment, that beyond a certain distance along the PmP branch, manual intervention was required to avoid cycle skipping. Further work on automatic phase picking of observed refraction data is still needed.

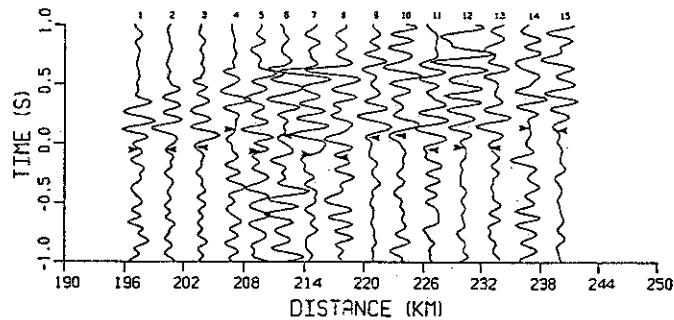


Figure 26.4 Automated correlation (picking) of refraction phases (Zelt *et al.*, 1987).

Recent examples of inversion for laterally varying structure using refraction travel times from controlled sources include Benz and Smith (1984), Elbring (1984), Kanasewich and Chiu (1985), Spence *et al.* (1985), Ankeny *et al.* (1986), Huang *et al.* (1986), White (1989), Hildebrand *et al.* (1989), White and Clowes (1990), Hawman *et al.* (1990), Lutter *et al.* (1990), and Zelt and Smith (1992). As one example of 2-D travel-time inversion, the results of Elbring (1984) are shown in Figure 26.5. Figure 26.5(a) shows three shot gathers along profile 9 of the 1980 Yellowstone–eastern Snake River Plain seismic experiment. Correlations of arrival times are also shown. The thick lines in Figure 26.5(b) show isovelocity contours of the inverted velocity model. The dots are the velocity node locations. Representative ray trajectories for all six shotpoints are also shown in Figure 26.5(b). The distribution of ray coverage gives qualitative information on which parts of the model are resolved by the data. The inversion results (Figure 26.5(b)) delineate a dramatic lateral change in seismic velocity in the upper 4 km of the model. The velocities decrease sharply to the south at the location of the boundary between Paleozoic sedimentary rocks and volcanics associated with the eastern Snake River Plain. The abrupt velocity transition is interpreted to be a fault (Figure 26.5(c)) consistent with the crustal model of Sparlin *et al.* (1982).

As a second example of 2-D inversion, Lutter *et al.* (1990) inverted for upper crustal structure using first arrival travel time data from the 1986 Ouachita PASSCAL experiment. The velocities were specified at nodes and interpolated by splines. The code SEIS83 was used for the ray-tracing (Červeny and Pšenčík, 1984) with the partial derivatives computed following Nowack and Lyslo (1989). An iterative linearized inversion was performed for the smoothly splined velocity nodes. Isovelocity contours of the inverted model for depths less than 9 km are displayed in Figure 26.6(b). The inversion procedure was iterated with rays traced in the updated model at each iteration. This procedure was continued until no significant improvement of travel time residuals was obtained. In order to stabilize the inversion, a set of iterative inversions was performed starting with a small number of widely spaced velocity nodes and then increasing the number of nodes. In this way, the longer wavelength features of the model were estimated first and then frozen into the model.

Figure 26.6(a) shows an independent geologic interpretation based on well log and other geologic information and compared with the inversion results in Figure 26.6(b) for depths above 9 km. Three distinct velocity gradients can be correlated with geologic units. Surface exposed Cretaceous and Jurassic sediments with velocities from 2 to 3.5 km s^{-1} extend to 1.5 km depth. Inferred Triassic rift fill sediments have inverted velocities ranging from 3.5 to 4.75 km s^{-1} between depths of 1.5 and 3.0 km. Finally,

Paleozoic sediments are imaged by a decreased velocity gradient below a depth of 3.0 km.

Lower resolution for depths greater than 12 km, using only first arrival travel times, necessitated the modeling of wide-angle reflected phases. Using reflected waves increases the regions of illumination as well as increasing angular ray coverage for the upper parts of the model. However, introducing interfaces adds a second type of medium parameter, depth to curved interfaces.

There have been several approaches to dealing with reflected arrivals. First, the interface shape and depth can be assumed a priori. Reflected travel times can then be used in a tomographic inversion for velocity alone. This approach was taken by Nercessian *et al.* (1984) who used reflections from the Moho to illuminate a shallower target. The second approach is to use velocities from a previous inversion and then invert for reflector shape. This approach was followed by Lutter and Nowack (1990) who used layer stripping to invert travel times for interfaces at progressively greater depth.

A third alternative in using reflected arrivals is to invert simultaneously for interfaces and velocities. In the seismic reflection geometry, this approach has been taken by Bishop *et al.* (1985), Stork and Clayton (1986), Farra and Madariaga (1988), and Williamson (1990). These studies show that care must be taken in such joint inversions. Farra and Madariaga (1988) allowed slownesses in each layer to vary only horizontally. Williamson (1990) used a multistage approach, in which successively shorter scale lengths were included. A simultaneous inversion for velocities and interfaces using refracted and wide-angle reflected travel times was presented by Zelt and Smith (1992) based on the forward modeling technique of Zelt and Ellis (1988).

A final alternative in using reflected arrivals is to alternate between imaging the reflectors by wavefield migration methods and imaging the velocities using a tomographic travel time inversion (Stork and Clayton, 1987; Bording *et al.*, 1987). This technique has the advantage of using more of the seismic wavefield data in the migration step. However, it has the disadvantage that two different types of data must be used for the inversion of the different model parameters.

Examples of inversions of refraction and wide-angle reflection data to obtain interface and velocity parameters are given by Chiu *et al.* (1986), Huang *et al.* (1986), Lutter and Nowack (1990), and Zelt and Smith (1992). Lutter and Nowack (1990) used wide-angle reflection travel times from the 1986 Ouachita PASSCAL experiment to image deep crustal reflectors. The travel times of wide-angle reflections were picked manually and checked with reciprocity of travel times between shot gathers. For the inversion, a layer stripping approach was taken where successively deeper interfaces were inverted while shallower structure was held fixed. The shallow crustal velocities were obtained from the first arrival travel time inversion of Lutter *et al.* (1990). The average velocities in the deeper layers were obtained using from τ - p and ray-trace analysis (Lutter and Nowack, 1990; Lyslo and Nowack, 1990). The crustal interfaces were then inverted at sequentially greater depths using reflected arrival times.

Figure 26.7 shows inversions for the top of the lower crustal layer as well as the Moho. For each interface, the observed and predicted travel times are shown, as well as the ray diagrams and the lateral resolution along the interface. Each interface is parameterized using bicubic splines to give smoothly curved boundaries. The resulting model is shown in Figure 26.8, incorporating both inverted upper crustal velocities and deeper interface depths. Inversion results for the central and southern portion of the profile indicate a depth of 10–12 km for a mid-crustal layer, a lower crustal layer with

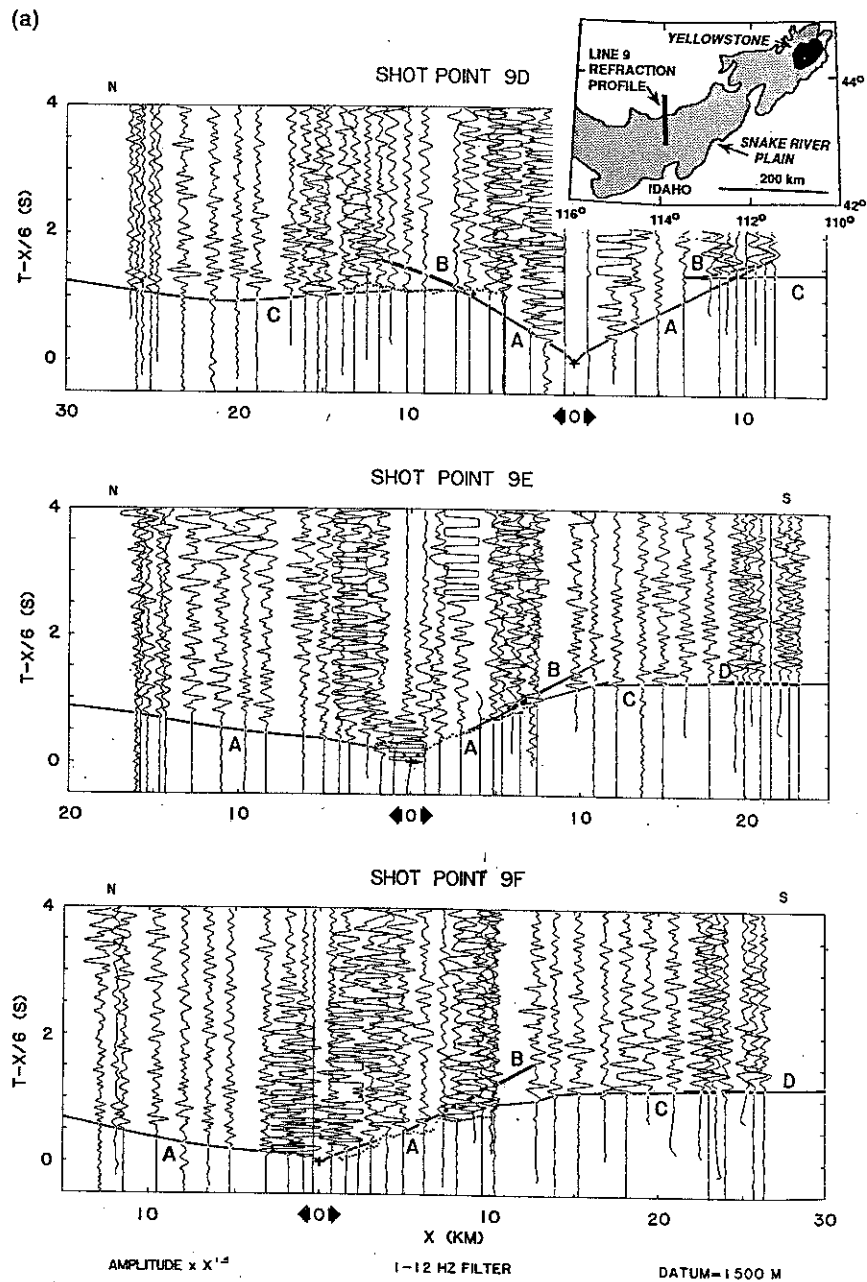


Figure 26.5 (a) Three shot gathers and travel time correlations for three of the line 9 record sections from the 1980 Yellowstone-eastern Snake River Plain seismic refraction experiment. An index map indicating the location of the profile is shown in the upper right. Seismograms are vertical component records. (b) Velocity contours (thick lines) of the inversion results. Velocity node points are shown as dots. Representative ray trajectories in the final model are also shown. (c) A geologic interpretation of the derived velocity model. (Adapted from Elbring, 1984.)

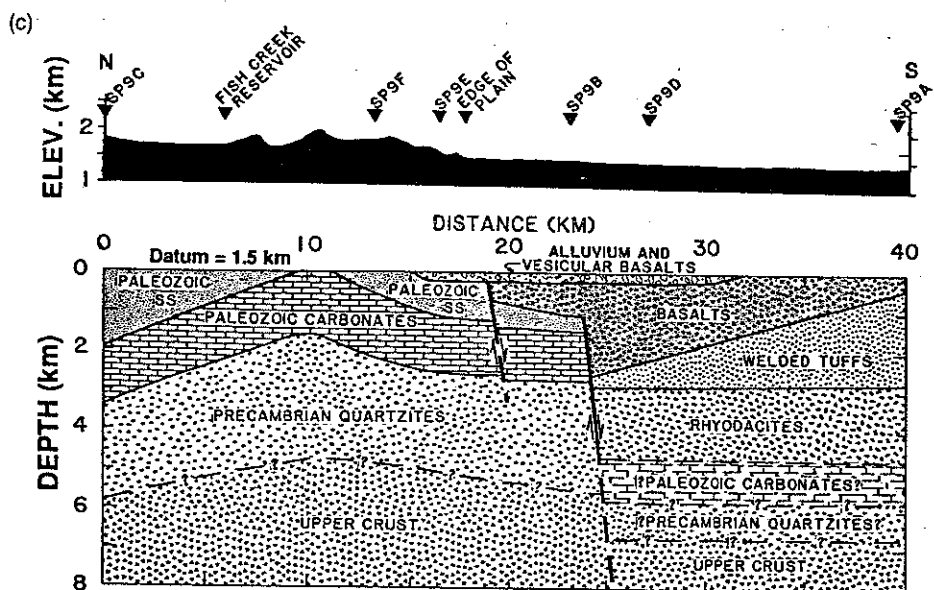
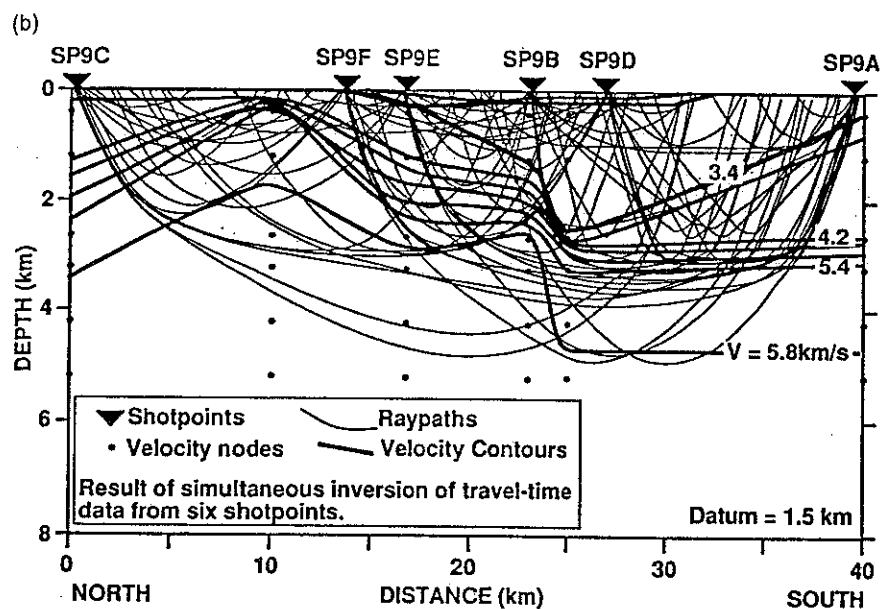


Figure 26.5 - contd.

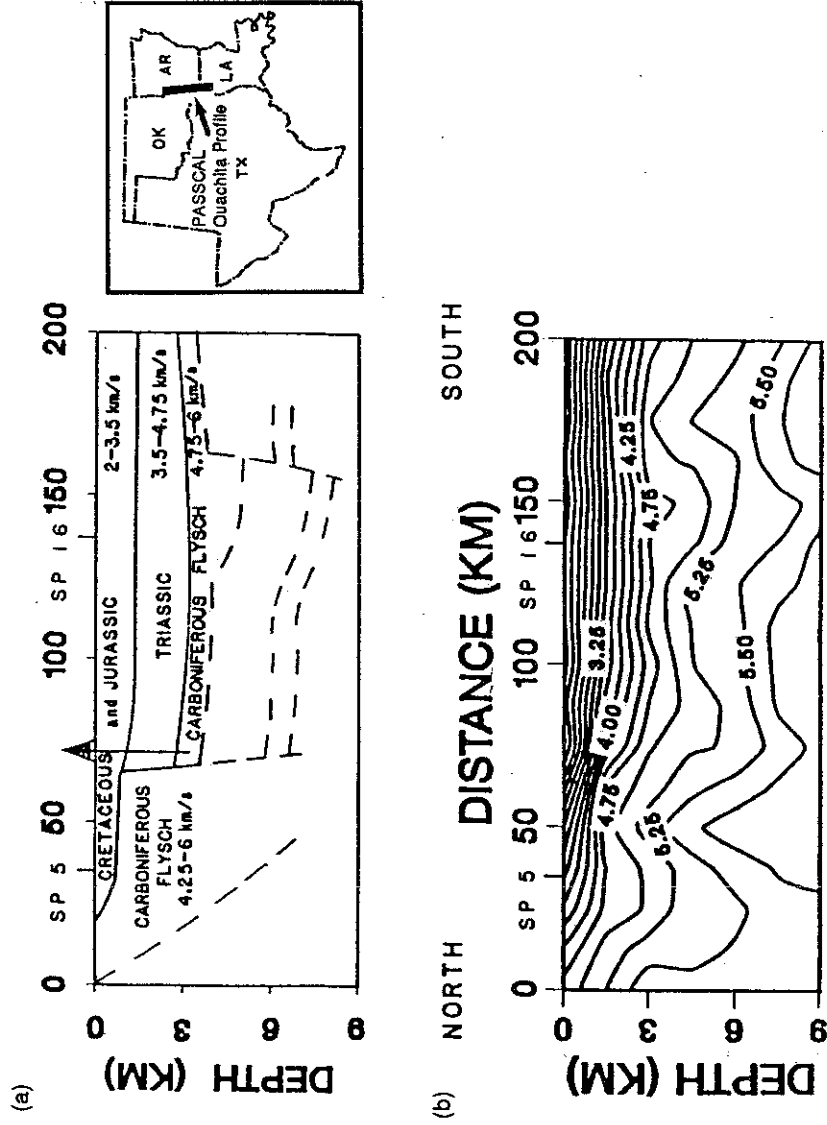


Figure 26.6 (a) Geologic structure for the upper crust along the 1986 Ouachita PASSCAL seismic profile based on well log data and other geologic information (Woods and Addington, 1973). Index map indicates location of the profile. (b) Upper crustal isovelocity contours from inversion of first arrival travel times from the Ouachita PASSCAL experiment (Lutter *et al.*, 1990).

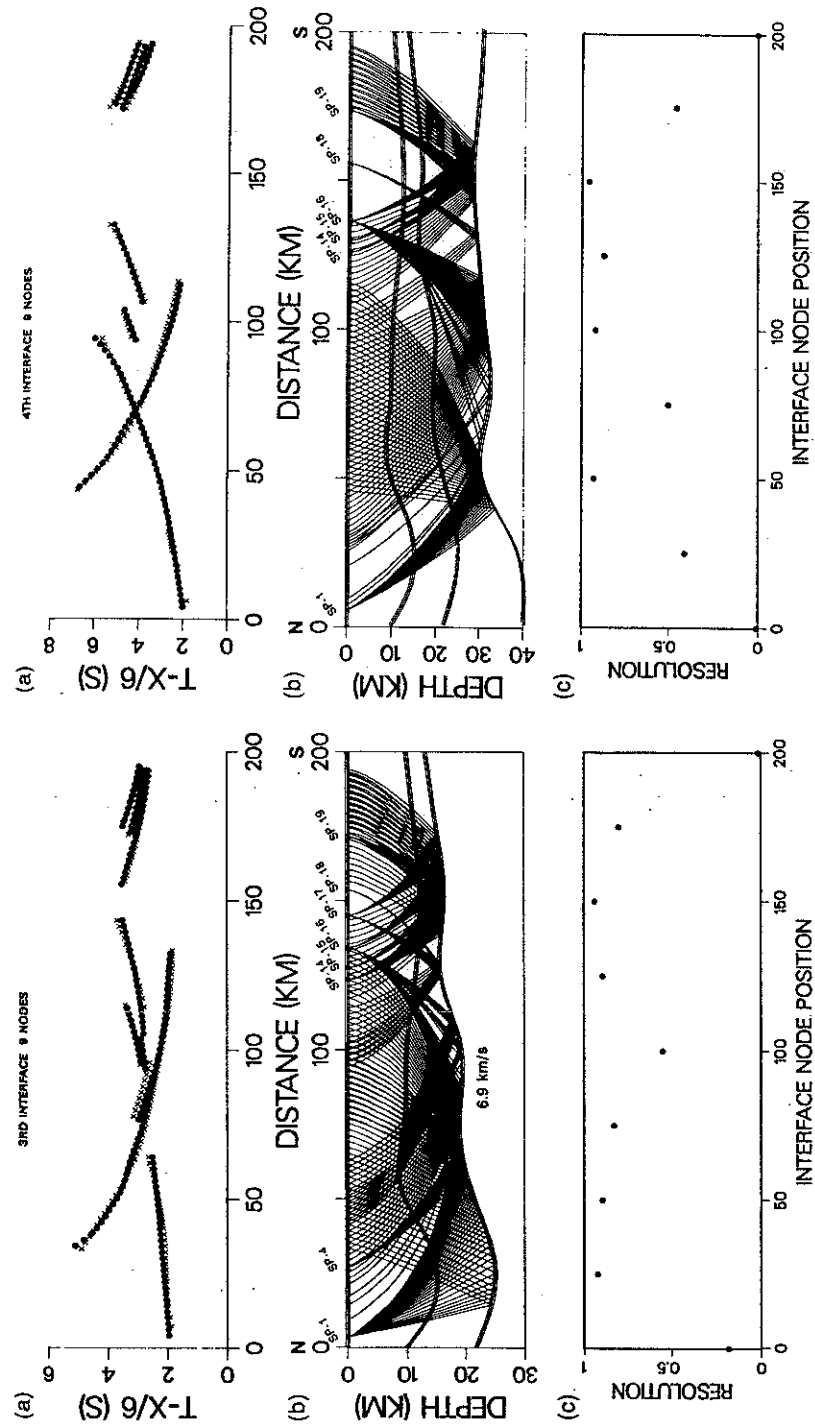


Figure 26.7 Inversion for deep crustal interfaces from the 1986 Ouachita PASSCAL experiment. Results for an intermediate depth crustal interface are shown on the left, and those for the Moho are shown on the right. For each interface, (a) shows the observed and calculated reflection travel times, (b) shows the interface model and ray diagram, and (c) shows the diagonals of the resolution matrix along each interface (Lutter and Nowack, 1990).

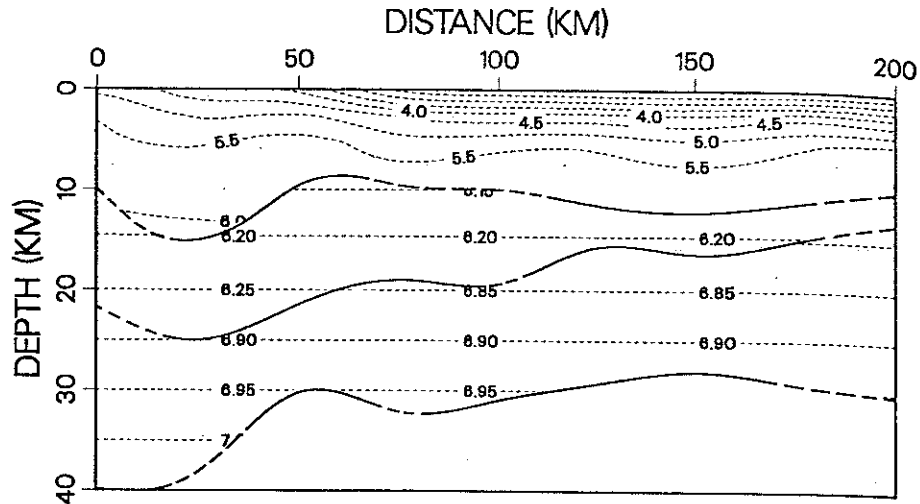


Figure 26.8 Velocity and interface model from inversion of first arrivals and wide-angle reflected arrivals of the 1986 Ouachita PASSCAL experiment. The distances are measured from the northern end of the line. Boundaries are dashed where diagonals of the resolution matrix are less than 0.5 (Lutter and Nowack, 1990).

an average thickness of 12 km, and a Moho depth of approximately 30 km. In the northern 50 km of the profile, the Moho shallows from 40 to 30 km.

Zelt and Smith (1992) provide a second example of the inversion of wide-angle data for velocity and interface parameters using data from the 1986 Nevada PASSCAL seismic experiment. Velocity parameters were defined by trapezoidal cells and interface parameters were linearly interpolated. Figure 26.9(a) shows a ray diagram for the PmP phase along the N-S profile of this experiment. Figure 26.9(b) shows a comparison of the observed and computed travel times. The observed travel times are shown by vertical bars indicating twice the estimated uncertainty of the pick. The computed travel times are shown by the solid curves. Figure 26.9(c) shows the inverted velocity and interface model for the N-S profile. The size of the solid squares gives the resolution of each interface node.

An example of elementary wavefield processing of wide-angle reflection data is given by Plappert (1987) for the 1986 Ouachita PASSCAL experiment. Plappert (1987) constructed a stacked equivalent zero-offset record section from wide-angle reflection data. The AGC corrected wavefield data were muted, normal move-out corrected, and then plotted at the mid-point distance between each source and receiver. The normal move-out correction was computed from a smoothly varying background velocity. The wavefield data from all shot gathers were processed in a similar manner and then binned into varying mid-point positions. Traces in different mid-point bins were then stacked to obtain the approximate zero-offset record sections. Figure 26.10 shows the middle part of the record section, from 80–180 km along the profile. The Moho can be seen at a depth of about 30 km. In addition, mid-crustal reflections can also be seen. See Figure 26.8 for a comparison with the travel time inversion results.

One issue that needs to be addressed in wavefield processing of wide-angle reflection data is the variation in amplitude from precritical to postcritical. For postcritical reflections, the reflection amplitude approaches unity and is, therefore, no longer

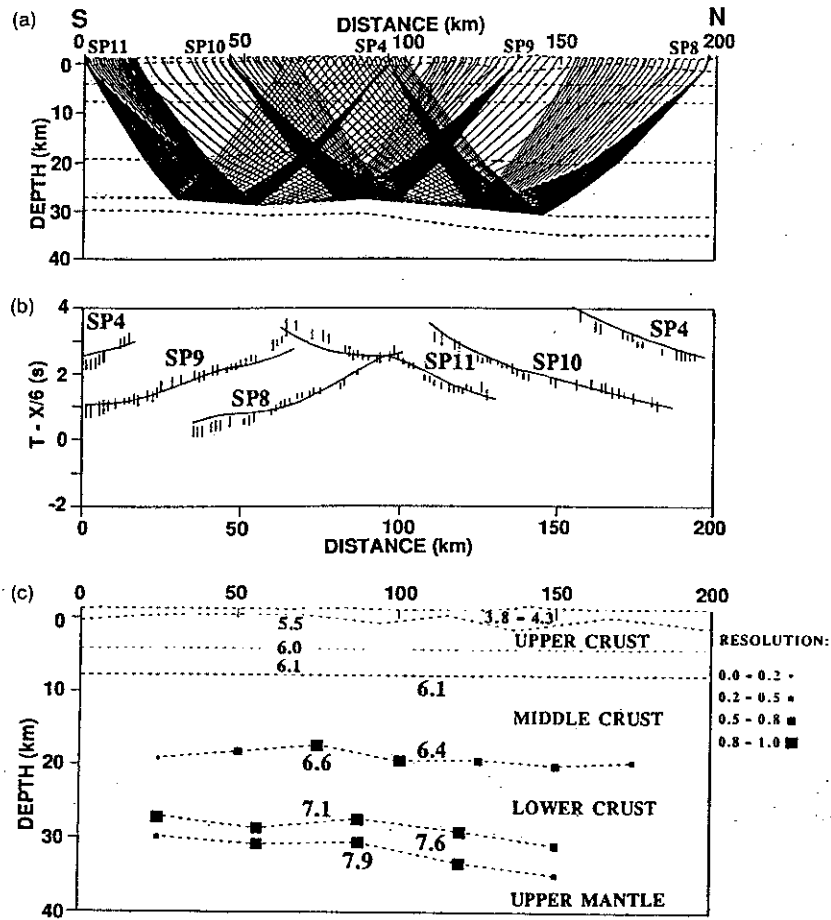


Figure 26.9 Inversion results for the N-S profile of the 1986 Nevada PASSCAL experiment from Zelt and Smith (1992). (a) Ray diagram for the PmP phase for the final velocity model. (b) Comparison of observed travel times, indicated by vertical bars giving twice the uncertainty of the pick, with calculated travel times, indicated by solid curves. (c) Resulting velocity and interface model. The sizes of the solid squares give the resolution of each interface node.

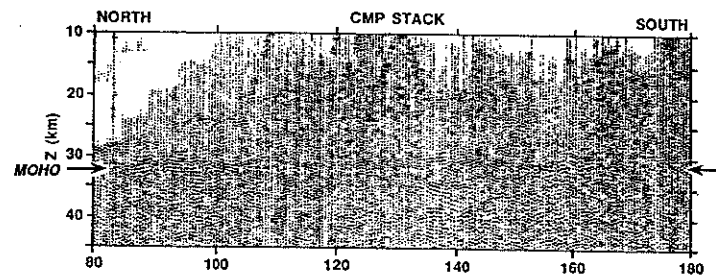


Figure 26.10 Wavefield processed wide-angle reflection data from the 1986 Ouachita PASSCAL experiment (Plappert, 1987). Central section of the profile 80-180 km from the northern end.

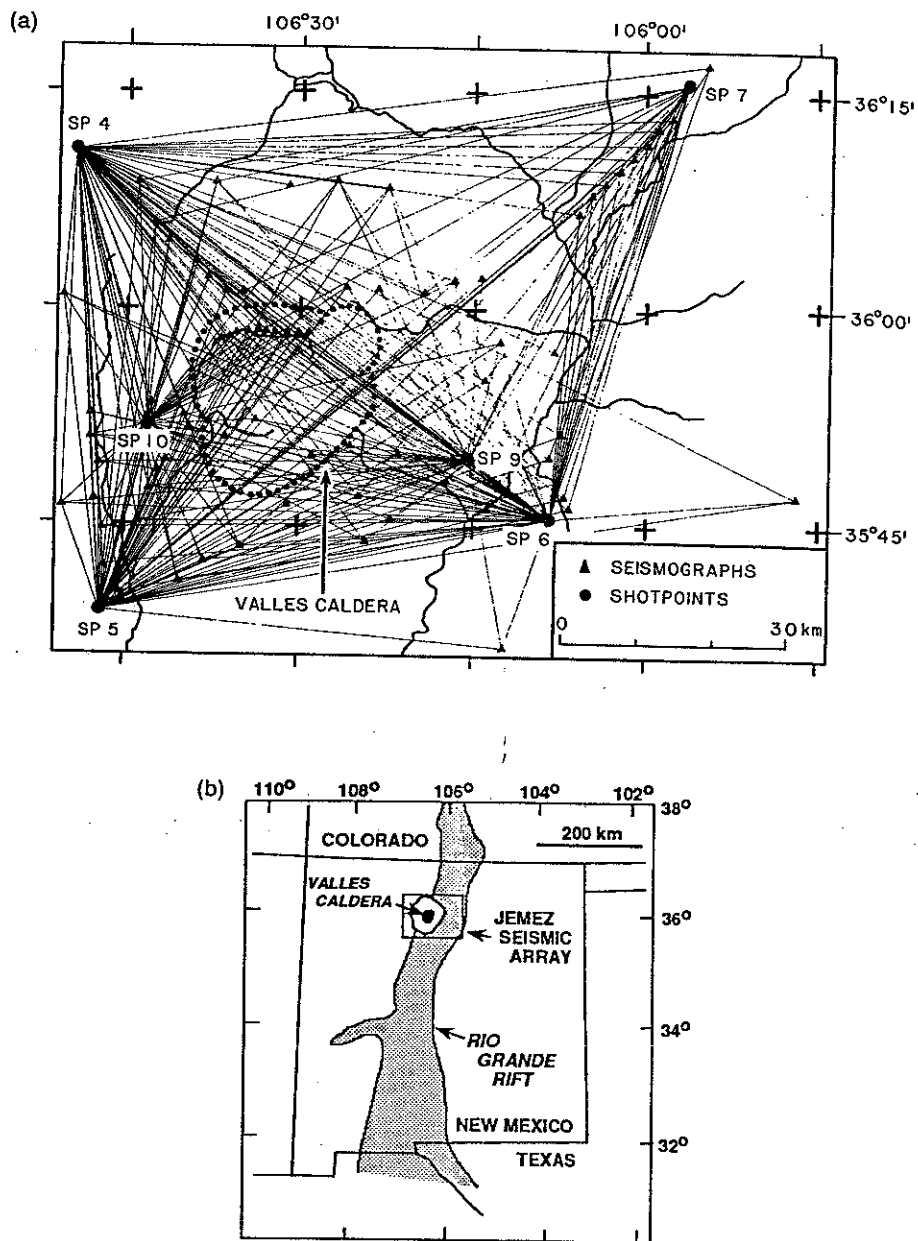


Figure 26.11 Three-dimensional refraction travel time inversion result for the upper crustal structure of the Jemez Mountains volcanic field, New Mexico (Ankeny *et al.*, 1986). (a) Map location of shotpoints (large dots), seismic stations (solid triangles), and ray-path coverage. (b) Index map showing location of shotpoints and recording stations illustrated in (a). (c) North-south and east-west cross-sections of the inverted velocity structure determined by 3-D inversion.

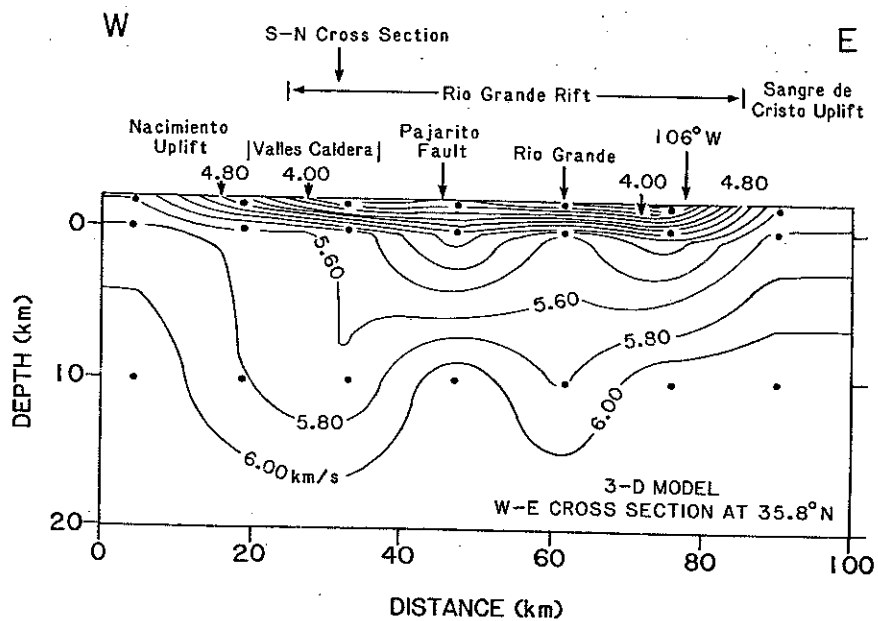
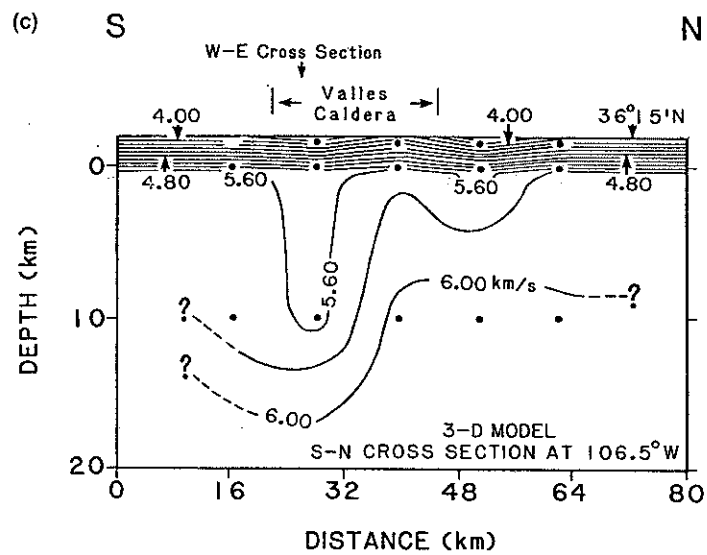


Figure 26.11 - contd.

proportional to the direct impedance contrast at the interface. However, the increase in amplitudes past the critical distance also gives rise to large postcritical signal strength. If there are no adjustments for variations in amplitude, wavefield processing of precritical and postcritical reflections will be biased toward the larger signal amplitudes. Further work on wavefield processing of wide-offset data for laterally varying structures is required.

Because the Earth is in reality three dimensional, 3-D seismic inversions are preferred. We present the work of Ankeny *et al.* (1986) as an example of a 3-D inversion of refraction data. Other examples are Thurber (1983), Benz and Smith (1984), and Thurber and Aki (1987). Ankeny *et al.* (1986) inverted for the upper crustal structure of the Jemez Mountains volcanic field, New Mexico using travel times from both explosions and earthquakes. Figure 26.11(a) shows a map location of the shot points, seismic stations, and ray-path coverage for the explosion data. Figure 26.11(c) shows N-S and E-W cross-sections through the velocity model determined by 3-D inversion. The two cross-sections display strong 3-D variations in the inverted velocity model.

The most prominent feature on the derived 3-D velocity model of the Jemez region is the zone of low ($5.6\text{--}5.8\text{ km s}^{-1}$) upper crustal velocities which extends to depths of about 10 km or more beneath the southern half of the Valles caldera. (Low velocities to the east beneath the Rio Grande rift are at least partially explained by rift fill and also extend into a region of the model where resolution is poorer due to limited source and receiver coverage). The low velocities beneath the Valles caldera are interpreted to be caused by the combined effects of a silicic intrusion in the upper crust and velocity reduction caused by elevated temperature (Ankeny *et al.*, 1986).

Further extensions and applications of refraction tomography include current work on the inversion for anisotropy (Hirahara and Ishikawa, 1984; Jech and Pšenčík, 1992), attenuation inversion using spectral ratios (Evans and Zucca, 1988), or amplitudes and pulse broadening (Nowack and Trehu, 1989), and simultaneous inversion of P and S travel times for shear velocity structure and Poisson's ratio (Holbrook *et al.*, 1988). In addition, further work on 3-D inversions using earthquake data and controlled sources is needed to invert simultaneously for hypocentral and subsurface medium parameters (Thurber, 1983, Chapter 20 of this volume; Sambridge, 1990).

26.5 CONCLUSIONS

The use of wide-angle seismic data has the advantage of a larger angular ray-path coverage as compared with other types of seismic data and can provide increased resolution of subsurface Earth structure. A number of inversion methods have been used to image wide-angle seismic data. These techniques are characterized by differing model complexity, model parameterization, source and receiver geometry, and solution method.

Recent applications of seismic tomography have emphasized the imaging of laterally varying structure which is of major importance in the geologic mapping of the Earth's interior. For smoothly varying media, ray-theoretical methods and their various extensions are applicable. Ray methods also can be applied to media with a small number of smoothly curved interfaces. Estimation of fine-scale structure of the subsurface is aided by full wavefield methods.

In the design of experiments for seismic imaging using refraction and wide-angle reflection data, recording geometries consisting of multiple sources and receivers and which result in many crossing ray-paths will provide better resolution of derived

velocity models. The increased resolution produced by favorable ray coverage pertains to both 2-D and 3-D models. However, the number of source and receiver locations required for the 3-D geometry is significantly greater. A few examples of 2-D and 3-D inversions from recent, mostly crustal structure, studies have been considered in this paper. In future experiments, significant improvements in capability to image velocity structure can be achieved with appropriate attention to design considerations (geometry and ray-path coverage). However, these design criteria will generally imply substantially increased observational effort – larger numbers of sources and receivers, and therefore, seismograms to be used in the tomographic inversion.

ACKNOWLEDGMENTS

The authors would like to thank H.M. Iyer for his encouragement, N.R. Gouly, and J.R. Evans for useful and constructive reviews, and C. Zelt and R. Smith for permission to use a figure from their paper. This work was supported by NSF grants EAR-8904169 and EAR-9018217 (R.L.N.) and NSF grants EAR-8642240/x and EAR-8817048 (L.W.B.).

REFERENCES

- Aki, K. and Lee, W.H.K. (1976) Determination of three-dimensional velocity anomalies under a seismic array using first P arrival times from local earthquakes. 1. A homogeneous initial model. *J. Geophys. Res.*, **81**, 4381–99.
- Aki, K. and Richards, P.G. (1980) *Quantitative Seismology, Theory and Methods*, W.H. Freeman, San Francisco.
- Alekseev, A.S., Lavrentiev, M.M., Mukhometov, R.G., *et al.* (1971) A numerical method of determination of the structure of the Earth's upper mantle, in *Mathematical Problems of Geophysics*, Vol. 2. (eds M.M. Lavrentiev and A.S. Alekseev), Computing Center, Academy of Science, U.S.S.R. (Siberian Branch), Novosibirsk; pp. 143–65 (in Russian).
- Alekseev, A.S., Lavrentiev, M.M., Romanov, V.G., *et al.* (1990) Theoretical and computational aspects of seismic tomography. *Surv. Geophys.*, **11**, 395–409.
- Allen, R. (1982) Automatic phase pickers: their present use and future prospects. *Bull. Seismol. Soc. Am.*, **72**, S225–42.
- Ankeny, L.A., Braile, L.W. and Olsen, K.H. (1986) Upper crustal structure beneath the Jemez Mountains Volcanic Field, New Mexico, determined by three-dimensional simultaneous inversion of seismic refraction and earthquake data. *J. Geophys. Res.*, **91**, 6188–98.
- Bamford, S. (1972) An example of the iterative approach to time-term analysis. *Geophys. J.R. Astron. Soc.*, **31**, 365–72.
- Benz, H.M. and Smith, R.B. (1984) Simultaneous inversion for lateral velocity variations and hypocenters in the Yellowstone region using earthquake and refraction data. *J. Geophys. Res.*, **89**, 1208–220.
- Bessonova, E.N., Fishman, V.M., Ryaboy, V.Z., *et al.* (1974) The tau method for inversion of travel times – I. deep seismic sounding data. *Geophys. J.R. Astron. Soc.*, **36**, 377–98.
- Beydoun, W.B. and Tarantola, A. (1988) First Born and Rytov approximations: modeling and inversion conditions in a canonical example. *J. Acoust. Soc. Am.*, **83**, 1045–55.
- Beylkin, G. (1984) The inversion problem and applications of the generalized Radon transform. *Commun. Pure Appl. Math.*, **37**, 579–99.
- Bishop, T.N., Bube, K.P., Cutler, R.T., *et al.* (1985) Tomographic determination of velocity and depth in laterally varying media. *Geophysics*, **50**, 903–23.
- Bording, R.P., Gerstenkorn, A., Lines, L.R., *et al.* (1987) Applications of seismic travel-time tomography. *Geophys. J. Int.*, **90**, 285–303.
- Braile, L.W. (1973) Inversion of crustal refraction and reflection data. *J. Geophys. Res.*, **78**, 7738–44.

- Braile, L.W. and Chiang, C.S. (1986) The continental Mohorovicic discontinuity: results from near-vertical and wide-angle seismic reflection studies, in *Reflection Seismology: The Global Perspective*, (eds M. Barazangi and L. Brown), AGU Geodynamic Series 13, Washington, D.C. pp. 257-72.
- Červený, V. (1985a) The application of ray tracing to the numerical modeling of seismic wavefields in complex structures, in *Seismic Shear Waves, Part A: Theory*, (ed. G. Dohr), Geophysical Press, London, pp. 1-124.
- Červený, V. (1985b) Gaussian beam synthetic seismograms. *J. Geophys.*, **58**, 44-72.
- Červený, V. (1985c) Ray synthetic seismograms for complex two dimensional and three dimensional structures. *J. Geophys.*, **58**, 2-26.
- Červený, V. (1987) Ray tracing algorithms in three-dimensional laterally varying layered structures, in *Seismic Tomography*, (ed. G. Nolet), Reidel, Hingham, MA, pp. 99-133.
- Červený, V. (1992) *Ray Methods for Three-dimensional Seismic Modelling, Lecture Notes*, University of Trondheim, Norway.
- Červený, V. and Fírbas, P. (1984) Numerical modelling and inversion of travel times of seismic body waves in inhomogeneous anisotropic media. *Geophys. J.R. Astron. Soc.*, **76**, 41-51.
- Červený, V. and Frangie, A.B. (1982) Effects of causal absorption on seismic body waves. *Stud. Geophys. Geod.*, **26**, 238-53.
- Červený, V. and Jech, J. (1982) Linearized solutions of kinematic problems of seismic body waves in inhomogeneous slightly anisotropic media. *J. Geophys.*, **51**, 96-104.
- Červený, V. and Pšenčík, I. (1984) SEIS83 - numerical modeling of seismic wave fields in 2-D Laterally varying structures by the ray method, in *Documentation of Earthquake Algorithms*, (ed. E.R. Engdahl), Report SE-15, World Data Center (A) for Solid Earth Geophysics, Boulder, CO, pp. 36-40.
- Červený, V., Klimes, L. and Pšenčík, I. (1988) Complete seismic ray tracing in three-dimensional structures, in *Seismological Algorithms*, (ed. D.J. Doornbos), Academic Press, San Diego, pp. 89-168.
- Červený, V., Popov, M.M. and Pšenčík, I. (1982) Computation of wave fields in inhomogeneous media - Gaussian beam approach. *Geophys. J.R. Astron. Soc.*, **70**, 109-28.
- Chang, W.F. and McMechan, G.A. (1989a) Wavefield processing of data from a large aperture experiment in southwestern Oklahoma. *J. Geophys. Res.*, **94**, 1803-16.
- Chang, W.F. and McMechan, G.A. (1989b) Wavefield processing of data from the 1986 Program for Array Seismic Studies of the Continental Lithosphere Ouachita experiment. *J. Geophys. Res.*, **94**, 17781-92.
- Chapman, C.H. (1981) Generalized Radon transforms and slant stacks. *Geophys. J.R. Astron. Soc.*, **66**, 445-53.
- Chapman, C.H. (1985) Ray theory and its extensions: WKBJ and Maslov seismograms. *J. Geophys.*, **58**, 27-43.
- Chapman, C.H. (1987) The Radon transform and seismic tomography, in *Seismic Tomography*, (ed. G. Nolet), Reidel, Hingham, MA, pp. 25-47.
- Chapman, C.H. and Drummond, R. (1982) Body-wave seismograms in inhomogeneous media using Maslov asymptotic theory. *Bull. Seismol. Soc. Am.*, **72**, S277-S317.
- Chapman, C.H. and Orcutt, J.A. (1985) Least-squares fitting of marine seismic refraction data. *Geophys. J.R. Astron. Soc.*, **82**, 339-74.
- Chiu, S.K.L., Kanasewich, E.R. and Phadke, S. (1986) Three-dimensional determination of structure and velocity by seismic tomography. *Geophysics*, **51**, 1559-71.
- Chou, C. and Booker, J. (1979) A Backus-Gilbert approach to inversion of travel time data for three-dimensional velocity structure. *Geophys. J.R. Astron. Soc.*, **59**, 325-44.
- Claerbout, J.F. (1971) Toward a unified theory of reflector mapping. *Geophysics*, **36**, 467-81.
- Claerbout, J.F. (1976) *Fundamentals of Geophysical Data Processing*, McGraw Hill, New York.
- Clayton, R.W. and McMechan, G.A. (1981) Inversion of refraction data by wave field continuation. *Geophysics*, **46**, 860-8.
- Crosson, R.S. (1976) Crustal structure modelling of earthquake data 1: simultaneous least squares estimation of hypocenter and velocity parameters. *J. Geophys. Res.*, **81**, 3036-46.

- Deans, S.R. (1983) *The Radon Transform and Some of its Applications*, Wiley Interscience, New York.
- Diebold, J.B. and Stoffa, P.L. (1981) The travel time equation, tau-p mapping and inversion of common midpoint data. *Geophysics*, **46**, 238–54.
- Dines, K.A. and Lytle, R.J. (1979) Computerized geophysical tomography. *Proc. IEEE*, **67**, 1065–73.
- Duijndam, A.J.W. (1988) Bayesian estimation in seismic inversion. Part 1: principles. *Geophys. Prospect.*, **36**, 878–98.
- Dziewonski, A.M. (1984) Mapping the lower mantle: determination of lateral heterogeneity in P velocity up to degree and order 6. *J. Geophys. Res.*, **89**, 5929–52.
- Elbring, G.J. (1984) *A Method for Inversion of Two Dimensional Seismic Refraction Data with Application to the Snake River Plain Region of Idaho*. Ph.D. Thesis, Purdue University, West Lafayette, In.
- Evans, J.R. and Zucca, J.J. (1988) Active high-resolution seismic tomography of compressional wave velocity and attenuation structure at Medicine Lake Volcano, Northern California Cascade Range. *J. Geophys. Res.*, **93**, 15 016–36.
- Farra, V. (1990) Amplitude computation in heterogeneous media by ray perturbation theory: a finite element approach. *Geophys. J. Int.*, **103**, 341–54.
- Farra, V. and Madariaga, R. (1987) Seismic waveform modeling in heterogeneous media by ray perturbation theory. *Geophys. J.R. Astron. Soc.*, **76**, 2697–712.
- Farra, V. and Madariaga, R. (1988) Non-linear reflection tomography. *Geophys. J.*, **95**, 135–47.
- Firbas, P. (1981) Inversion of travel-time data for laterally heterogeneous velocity structure – linearization approach. *Geophys. J.R. Astron. Soc.*, **67**, 189–98.
- Firbas, P. (1987) Tomography from seismic profiles, in *Seismic Tomography*, (ed. G. Nolet), Reidel, Hingham, MA, pp. 189–202.
- Flueh, E.R., Mooney, W.D., Fuis, G.S., *et al.* (1989) Crustal structure of the Chugach Mountains, Southern Alaska: a study of peg-leg multiples from a low velocity zone. *J. Geophys. Res.*, **94**, 16 023–35.
- Franklin, J.N. (1970) Well-posed stochastic extensions of ill-posed linear problems. *J. Math. Anal. Appl.*, **31**, 682–716.
- Gajewski, D. and Pšenčík, I. (1989) Computation of high-frequency seismic wavefields in 3-D laterally inhomogeneous anisotropic media. *Geophys. J.R. Astron. Soc.*, **91**, 383–412.
- Garmany, J., Orcutt, J.A. and Parker, R.L. (1979) Travel time inversion: a geometric approach. *J. Geophys. Res.*, **84**, 3615–22.
- Gerver, M. and Markushevich, V. (1967) On the characteristic properties of travel time curves. *Geophys. J.R. Astron. Soc.*, **13**, 241–46.
- Hanyga, A. (1982) The kinematic inverse problem for weakly laterally inhomogeneous anisotropic media. *Tectonophysics*, **90**, 253–62.
- Hawman, R.B., Colburn, R.H., Walker, D.A., *et al.* (1990) Processing and inversion of refraction and wide-angle reflection data from the 1986 Nevada PASSCAL experiment. *J. Geophys. Res.*, **95**, 4657–91.
- Healy, J.H. (1963) Crustal structure along the coast of California from seismic-refraction measurements. *J. Geophys. Res.*, **68**, 5777–87.
- Hearn, T.M. and Clayton, R.W. (1986) Lateral velocity variations in southern California. I. Results for the upper crust from Pg waves. *Bull. Seismol. Soc. Am.*, **76**, 495–509.
- Herglotz, G. (1907) Über das benndorfsche Problem der Fortpflanzungsgeschwindigkeit der Erdbebenstrahlen. *Z. Geophys.*, **8**, 145–7.
- Herman, G.T. (1980) *Image Reconstruction from Projections*. Academic Press, New York.
- Hildebrand, J.A., Dorman, L.M., Hammer, P.T.C., *et al.* (1989) Seismic tomography of Jasper Seamount. *Geophys. Res. Lett.*, **16**, 1355–8.
- Hirahara, K. and Ishikawa, Y. (1984) Travel-time inversion for three-dimensional P-wave velocity anisotropy. *J. Phys. Earth*, **32**, 197–218.
- Holbrook, W.S., Gajewski, D., Krammer, A., *et al.* (1988) An interpretation of wide-angle compressional and shear wave data in southwest Germany: Poisson's ratio and petrological implications. *J. Geophys. Res.*, **93**, 12 081–106.

- Huang, H., Spencer, C. and Green, A. (1986) A method for the inversion of refraction and reflection travel times for laterally varying velocity structure. *Bull. Seismol. Soc. Am.*, **76**, 837–46.
- Jackson, D.D. (1972) Interpretation of inaccurate, insufficient, and inconsistent data. *Geophys. J.R. Astron. Soc.*, **28**, 97–109.
- Jackson, D.D. and Matsu'ura, M. (1985) A Bayesian approach to nonlinear inversion. *J. Geophys. Res.*, **90**, 581–91.
- Jacobson, R.S. and Lewis, B.T.R. (1990) The first direct measurements of upper oceanic crustal compressional wave attenuation. *J. Geophys. Res.*, **95**, 17 417–30.
- Jarchow, C.M., Goodwin, E.B. and Catchings, R.D. (1990) Are large explosive sources applicable to resource exploration? *The Leading Edge*, **9**, 12–17.
- Jardine, W.G. (1988) *Seismic Reflection–Refraction Study over the Southern Margin of the Ouachita System of Arkansas and the Adjacent Gulf Coastal Plain*. M.Sc. Thesis, Purdue University, West Lafayette, IN.
- Jech, J. and Pšenčík, I. (1989) First order perturbation method for anisotropic media. *Geophys. J. Int.*, **99**, 369–76.
- Jech, J. and Pšenčík, I. (1992) Kinematic inversion for qP and qS waves in inhomogeneous anisotropic structures. *Geophys. J. Int.*, **108**, 604–12.
- Kanasewich, E.R. and Chiu, S.K.L. (1985) Least-squares inversion of spatial seismic refraction data. *Bull. Seismol. Soc. Am.*, **75**, 865–80.
- Keller, G.R., Braile, L.W., McMechan, G.A., *et al.* (1989) Crustal structure of the Ouachita orogenic belt determined by a PASSCAL wide-angle reflection/refraction experiment. *Geology*, **17**, 119–22.
- Keller, J.B. (1969) Accuracy and validity of the Born and Rytov approximations. *J. Opt. Soc. Am.*, **59**, 1003–4.
- Kennett, B.L.N. (1976) A comparison of travel time inversions. *Geophys. J.R. Astron. Soc.*, **44**, 517–36.
- Kennett, B.L.N. and Orcutt, J.A. (1976) A comparison of travel time inversions for marine refraction profiles. *J. Geophys. Res.*, **81**, 4061–70.
- Kennett, B.L.N. and Williamson, P.R. (1988) Subspace methods for large-scale nonlinear inversion, in *Mathematical Geophysics*, (eds N.J. Vlaar, G. Nolet, M.J.R. Wortel, *et al.*), Reidel, Hingham, MA, pp. 139–54.
- Kissling, E. (1988) Geotomography with local earthquake data. *Rev. Geophys.*, **26**, 659–98.
- Klem-Musatov, K.D. and Aizenberg, A.M. (1984) The ray method and the theory of edge waves. *Geophys. J.R. Astron. Soc.*, **79**, 35–50.
- Kravtsov, Y.A. and Orlov, Y.I. (1990) *Geometric Optics of Inhomogeneous Media*, Springer Verlag, Berlin.
- Lanczos, C. (1961) *Linear Differential Operators*, Van Nostrand, New York.
- Lutter, W.J. and Nowack, R.L. (1990) Inversion for crustal structure using reflections from the PASSCAL Ouachita experiment. *J. Geophys. Res.*, **95**, 4633–46.
- Lutter, W.J., Nowack, R.L. and Braile, L.W. (1990) Seismic imaging of upper crustal structure using travel times from the PASSCAL Ouachita experiment. *J. Geophys. Res.*, **95**, 4621–31.
- Lyslo, J.A. (1988) *Seismic Velocity Analysis of Shot Point 16 from the PASSCAL Ouachita Experiment*. M.Sc. Thesis, Purdue University, West Lafayette, IN.
- Lyslo, J.A. and Nowack, R.L. (1990) Slant stack velocity analysis of shot point 16 from the 1986 PASSCAL Ouachita experiment. *J. Geophys. Res.*, **95**, 4647–56.
- Macdonald, C., Davis, P.M. and Jackson, D.D. (1987) Inversion of reflection travel times and amplitudes. *Geophysics*, **52**, 606–17.
- McMechan, G.A. and Fuis, G.S. (1987) Ray equation migration of wide angle reflections from southern Alaska. *J. Geophys. Res.*, **92**, 407–20.
- McMechan, G.A. and Ottolini, R. (1980) Direct observation of a p-tau curve in a slant stacked wavefield. *Bull. Seismol. Soc. Am.*, **70**, 775–89.
- Moczo, P., Bard, P.Y. and Pšenčík, I. (1987) Seismic response of two-dimensional absorbing structures by the ray method. *J. Geophys.*, **62**, 38–49.
- Nercessian, A., Hirn, A. and Tarantola, A. (1984) Three-dimensional seismic prospecting of the Mont Dore volcano, France. *Geophys. J.R. Astron. Soc.*, **76**, 307–15.

- Nolet, G. (1985) Solving or resolving inadequate and noisy tomographic systems. *J. Comput. Phys.*, **61**, 463–82.
- Nolet, G. (1987) Seismic wave propagation and seismic tomography, in *Seismic Tomography*, (ed. G. Nolet), Reidel, Hingham, MA, pp. 1–14.
- Novotny, M. (1981) Two methods of solving the linearized two-dimensional inverse seismic kinematic problem. *J. Geophys.*, **50**, 7–15.
- Nowack, R.L. (1990) Tomography and the Herglotz–Wiechert inverse formulation. *Pure Appl. Geophys.*, **133**, 305–15.
- Nowack, R.L. (1992) Wavefronts and solutions of the eikonal equation. *Geophys. J. Int.*, **110**, 55–62.
- Nowack, R.L. and Aki, K. (1984) The 2-D Gaussian beam method: testing and application. *J. Geophys. Res.*, **89**, 7797–819.
- Nowack, R.L. and Aki, K. (1986) Iterative inversion for velocity using waveform data. *Geophys. J.R. Astron. Soc.*, **87**, 701–30.
- Nowack, R.L. and Lutter, W.J. (1988a) Linearized rays, amplitude and inversion. *Pure Appl. Geophys.*, **128**, 401–21.
- Nowack, R.L. and Lutter, W.J. (1988b) A note on the calculation of covariance and resolution. *Geophys. J.*, **95**, 205–7.
- Nowack, R.L. and Lyslo, J.A. (1989) Frechet derivatives for curved interfaces in the ray approximation. *Geophys. J. Int.*, **97**, 497–509.
- Nowack, R.L. and Pšencik, I. (1991) Perturbation from isotropic to anisotropic heterogeneous media in the ray approximation. *Geophys. J. Int.*, **106**, 1–10.
- Nowack, R.L. and Trehu, A.M. (1989) Simultaneous inversion for focusing and attenuation. *Eos, Trans. Am. Geophys. Union*, **70**, 1214.
- Ocola, L. (1972) A nonlinear least-squares method for seismic refraction mapping. *Geophysics*, **37**, 273–87.
- Orcutt, J.A. (1980) Joint linear, extremal inversion of seismic kinematic data. *J. Geophys. Res.*, **85**, 2646–60.
- Oristaglio, M.L. (1985) Accuracy of the Born and Rytov approximations for reflection and refraction at a plane interface. *J. Opt. Soc. Am. A*, **2**, 1987–993.
- Paige, C.C. and Saunders, M.A. (1982) LSQR: an algorithm for sparse linear equations and sparse least squares. *ACM Trans. Math. Software*, **8**, 43–71.
- Pan, G.S. and Phinney, R.A. (1989) Full-waveform inversion of plane-wave seismograms in stratified acoustic media: applicability and limitations. *Geophysics*, **54**, 368–80.
- Pavlis, G.L. and Booker, J.R. (1980) The mixed discrete–continuous inverse problem: application to the simultaneous determination of earthquake hypocenters and velocity structure. *J. Geophys. Res.*, **85**, 4801–10.
- Pedersen, H.M., Gelius, L.J. and Stamnes, J.J. (1989) 3D seismic modelling of edge diffractions. *Geophys. Prospect.*, **37**, 639–46.
- Phinney, R.A., Chowdhury, K.R. and Frazer, L.N. (1981) Transformation and analysis of record sections. *J. Geophys. Res.*, **86**, 359–77.
- Plappert, J.W. (1987) *Processing and Interpretation of Near Vertical and Wide Angle Seismic Reflection Data from the PASSCAL Ouachita Lithospheric Seismic Study*. M.Sc. Thesis, Purdue University, West Lafayette, IN.
- Popov, M.M. (1982) A new method of computation of wave fields using Gaussian beams. *Wave Motion*, **4**, 85–97.
- Raitt, R.W., Shor, G.G., Francis, T.J.G., et al. (1969) Anisotropy of the Pacific upper mantle. *J. Geophys. Res.*, **74**, 3095–109.
- Romanov, V.G. (1974) *Integral Geometry and Inverse Problems for Hyperbolic Equations*, Springer Tracts, 26, Springer-Verlag, New York.
- Romanov, M.E. and Alekseev, A.S. (1980) A characteristic method for numerical solution of the inverse kinematic seismic problems. *J. Geophys.*, **48**, 173–80.
- Sambridge, M.S. (1990) Non-linear arrival time inversion: constraining velocity anomalies by seeking smooth models in 3-D. *Geophys. J. Int.*, **102**, 653–77.

- Scheidegger, A.E. and Willmore, P.L. (1957) The use of a least squares method for the interpretation of data from seismic surveys. *Geophysics*, **22**, 9–22.
- Shaw, P.R. (1988) Waveform inversion of time-corrected refraction data. *Geophys. J.*, **93**, 75–90.
- Shaw, P.R. and Orcutt, J.A. (1985) Waveform inversion of seismic refraction data and applications to young Pacific crust. *Geophys. J.R. Astron. Soc.*, **82**, 375–414.
- Slichter, L.B. (1932) The theory of the interpretation of seismic travel time curves in horizontal structures. *Physics*, **6**, 273–95.
- Spakman, W. and Nolet, G. (1988) Imaging algorithms, accuracy and resolution in delay time tomography, in *Mathematical Geophysics*, (eds N.J. Vlaar, G. Nolet, M.J.R. Wortel, *et al.*) Reidel, Hingham, MA, pp. 155–87.
- Sparlin, M.A., Braile, L.W. and Smith, R.B. (1982) Crustal structure of the eastern Snake River Plain determined from ray trace modeling of seismic refraction data. *J. Geophys. Res.*, **87**, 2619–33.
- Spence, G.D., Clowes, R.M. and Ellis, R.M. (1985) Seismic structure across the active subduction zone of western Canada. *J. Geophys. Res.*, **90**, 6754–72.
- Stoffa, P.L. (ed.) (1989) *Tau-P: A Plane Wave Approach to the Analysis of Seismic Data*, Kluwer Academic Publishers, Dordrecht, Holland.
- Stoffa, P.L., Buhl, P., Diebold, J.B., *et al.* (1981) Direct mapping of seismic data to the domain of intercept and ray parameter – a plane wave decomposition. *Geophysics*, **46**, 255–67.
- Stork, C. and Clayton, R.W. (1986) Analysis of the resolution between ambiguous velocity and reflector position for travel time tomography, in *Extended Abstracts, 56th SEG International Meeting*, Houston, 2–6 November 1986, SEG, Tulsa, pp. 545–50.
- Stork, C. and Clayton, R.W. (1987) Application of tomography to two data sets containing lateral velocity variations, in *Extended Abstracts, 57th SEG International Meetings*, New Orleans, 11–15 October 1987, SEG, Tulsa, pp. 839–42.
- Sun, R. and McMechan, G.A. (1991) Full-wavefield inversion of wide-aperture SH and Love wave data. *Geophys. J. Int.*, **106**, 67–76.
- Tarantola, A. (1984) Inversion of seismic reflection data in the acoustic approximation. *Geophysics*, **49**, 1259–66.
- Tarantola, A. (1987) *Inverse Problem Theory: Methods for Data Fitting and Model Parameter Estimation*, Elsevier, Amsterdam.
- Tarantola, A. and Valette, B. (1982) Generalized non-linear inverse problems solved using the least squares criterion. *Rev. Geophys. Space Phys.*, **20**, 219–32.
- Thompson, C.J. and Chapman, C.H. (1985) An introduction to Maslov's asymptotic method. *Geophys. J.R. Astron. Soc.*, **61**, 729–46.
- Thurber, C.H. (1983) Earthquake locations and three-dimensional crustal structure in the Coyote Lake Area, Central California. *J. Geophys. Res.*, **88**, 8226–36.
- Thurber, C.H. and Aki, K. (1987) Three-dimensional seismic imaging. *Annu. Rev. Earth Planet. Sci.*, **15**, 115–39.
- Tonn, R. (1991) The determination of the seismic quality factor Q from VSP data: a comparison of different computational methods. *Geophys. Prospect.*, **39**, 1–27.
- Van der Sluis, A. and Van der Vorst, H.A. (1987) Numerical solution of large, sparse linear systems arising from tomographic problems, in *Seismic Tomography*, (ed. G. Nolet), Reidel, Hingham, MA, pp. 53–87.
- Vest, C.M. (1974) Formation of images from projections: Radon and Abel transforms. *J. Opt. Soc. Am.*, **64**, 1215–18.
- Vidale, J. (1988) Finite-difference calculation of travel times. *Bull. Seismol. Soc. Am.*, **78**, 2062–76.
- Virieux, J. (1991) Fast and accurate ray tracing by Hamiltonian perturbation. *J. Geophys. Res.*, **96**, 579–94.
- Virieux, J., Farra, V. and Madariaga, R. (1988) Ray tracing in laterally heterogeneous media for earthquake location. *J. Geophys. Res.*, **93**, 6585–99.
- Wesson, R.L. (1971) Travel time inversion for laterally inhomogeneous crustal velocity models. *Bull. Seismol. Soc. Am.*, **61**, 729–46.

- White, D.J. (1989) Two-dimensional seismic refraction tomography. *Geophys. J.*, **97**, 223–45.
- White, D.J. and Clowes, R.M. (1990) Shallow crustal structure beneath the Juan de Fuca Ridge from 2-D seismic refraction tomography. *Geophys. J. Int.*, **100**, 349–67.
- Wiechert, E. (1910) Bestimmung des Weges der Erdbebenwellen im Erdinnern. I. Theoretisches. *Phys. Z.*, **11**, 294–304.
- Wiggins, R.A. (1972) General linear inverse problem – implication of surface waves and free oscillations for earth structure. *Rev. Geophys. Space. Phys.*, **10**, 251–85.
- Williamson, P.R. (1990) Tomographic inversion in reflection seismology. *Geophys. J. Int.*, **100**, 255–74.
- Williamson, P.R. (1991) A guide to the limits of resolution imposed by scattering in ray tomography. *Geophysics*, **56**, 202–7.
- Willmore, P.L. and Bancroft, A.M. (1960) The time term approach to refraction seismology. *Geophys. J.R. Astron. Soc.*, **3**, 419–32.
- Woods, R.D. and Addington, J.W. (1973) Pre-Jurassic geologic framework northern Gulf basin. *Trans. Gulf Coast Assoc. Geol. Soc.*, **23**, 92–108.
- Zelt, C.A. and Ellis, R.M. (1988) Practical and efficient ray tracing in two-dimensional media for rapid traveltimes and amplitude forward modelling. *Can. J. Expl. Geophys.*, **24**, 16–31.
- Zelt, C.A. and Smith, R.B. (1992) Seismic traveltime inversion for 2-D crustal velocity structure. *Geophys. J. Int.*, **108**, 16–34.
- Zelt, C.A., Drew, J.J., Yedlin, M.J., *et al.* (1987) Picking noisy refraction data using semblance supplemented by a Monte Carlo procedure and spectral balancing. *Bull. Seismol. Soc. Am.*, **77**, 942–57.